

STUDY OF THE EFFECTS OF HEAT-INPUT ON MICROSTRUCTURE & GRAIN SIZE OF SUBMERGED ARC WELDING (SAW) WELDS BY DIGITAL IMAGE ANALYSIS TECHNIQUE

A MAJOR PROJECT SUBMITTED TO THE FACULTY OF TECHNOLOGY,
UNIVERSITY OF DELHI, NEW DELHI

TOWARDS THE PARTIAL FULLFILMENT OF
THE AWARD OF MASTER OF ENGINEERING
IN
PRODUCTION ENGINEERING

Submitted by

SANDIP KUMAR CHOUDHARY
(Roll No. 02/ME (P)/03)

*Under the guidance
of*

PROF. C.K. DUTTA



DEPARTMENT OF MECHNICAL / PRODUCTION ENGINEERING
DELHI COLLEGE OF ENGINEERING
UNIVERSITY OF DELHI
NEW DELHI

<http://www.dceonline.net>, <http://www.dce.edu>

CERTIFICATE

This is to certify that **SANDIP KUMAR CHOUDHARY** of Master of Engineering in 'PRODUCTION ENGINEERING' of Delhi College of Engineering, bearing Roll No. 02/ME (P)/03 has individually completed a project entitled "Study of the effects of Heat -input on microstructure and grain size of SAW welds by digital image analysis technique" under the prominent guidelines of **Prof. C. K. DUTTA**, Professor, Department of Production/ Mechanical Engg., Delhi College of Engineering, New Delhi. To the best of my knowledge and belief, this work has not been submitted to any other university or institution for the award of any degree or diploma.

He bears a good moral character, and we wish him all success in his life.

The project work has been carried out from... August'04

Prof. C. K. Dutta

Professor,
Department of Mechanical/
Production Engineering
Delhi College of Engineering,
New Delhi - 110042

ACKNOWLEDGEMENT

I am grateful to my individuals to many who made their time and knowledge available to help to work on “**Study of the effects of heat input on microstructure and grain size of SAW welds by digital image analysis technique**”.

Firstly I sincerely express deep sense of gratitude to my guide **Prof. C. K. Dutta**, Professor, Department of Mechanical/Production Engineering Delhi College of Engineering, University of Delhi, Delhi, for his kind discussion, support, co-operation and guidance.

I am also thankful to **Prof. S. Maji**, Head of the Department of Mechanical/Production Engineering, Delhi College of Engineering, Delhi for giving me permission to do project work at DCE Workshop, New Delhi.

I am also thankful to **Mr. Ajay Kishore**, **Mr. Vinay Kumar**, Lab assistant, Welding Lab, Delhi College of Engineering, New Delhi and **Mr. Sandeep** for extending the laboratory facilities during my project tenure.

I am also thankful to **Mr. Raj Kumar Singh**, **Mr. Prince Bovas**, Research Scholar, **Mr. Kishore Kolhe**, **Mr. Siddarth**, **Mr. Mohan Kumar**, **Mr. Jitendra Pandey** and rest of the member of the lab for their kind help, moral support and inspiration.

I express my gratitude to my parents, brothers, Sister and friends for their kind help and continuous encouragement during my project work.

Contents

1. INTRODUCTION

1.1	Introduction	1
1.2	Process	4
1.2.1	Nomenclature of Weld bead	9
1.3	SAW Fluxes	9
1.3.1	Classification of Fluxes	9
1.4	Operating Variables	14
1.4.1	Welding Current	14
1.4.2	Arc Voltage	15
1.4.3	Travel Speed	16
1.4.4	Size of the electrode	17
1.4.5	Electrode sickouts	17
1.4.6	Plate thickness	18
1.4.7	Heat input rate	18
1.5	Advantages	19
1.6	Limitations	19
1.7	Applications	20
1.8	Properties of the weld metal	21
1.9	Weld metal microconstituents	21
1.10	Types of grain exist in weldment	27
1.11	Objective of present work	28

2. EXPERIMENTATION	29
2.1 Welding Equipment	29
2.2 Base material	30
2.3 Consumables	30
2.3.1 Filler wire	30
2.3.2 Fluxes	30
2.4 WorkStation used for Image analysis consisting	31
2.5 Software used	31
2.6 Steps of Experiment	36
2.7 Experimental procedure	37
3. RESULTS & DISCUSSIONS	
Influence of increasing the heat input on microstructure, grain	
Size and thus on hardness.	38
3.1.1 Influence of increasing the welding current on phases	38
3.1.2. Effect of increasing the arc voltage on phases	52
3.2.1 Influence of increasing the welding current on grain size	68
3.2.2 Effect of increasing the arc voltage on grain size	73
4. CONCLUSIONS	78
5. SCOPE FOR THE FUTURE WORK	79
6. REFERENCES	80



1.1 INTRODUCTION

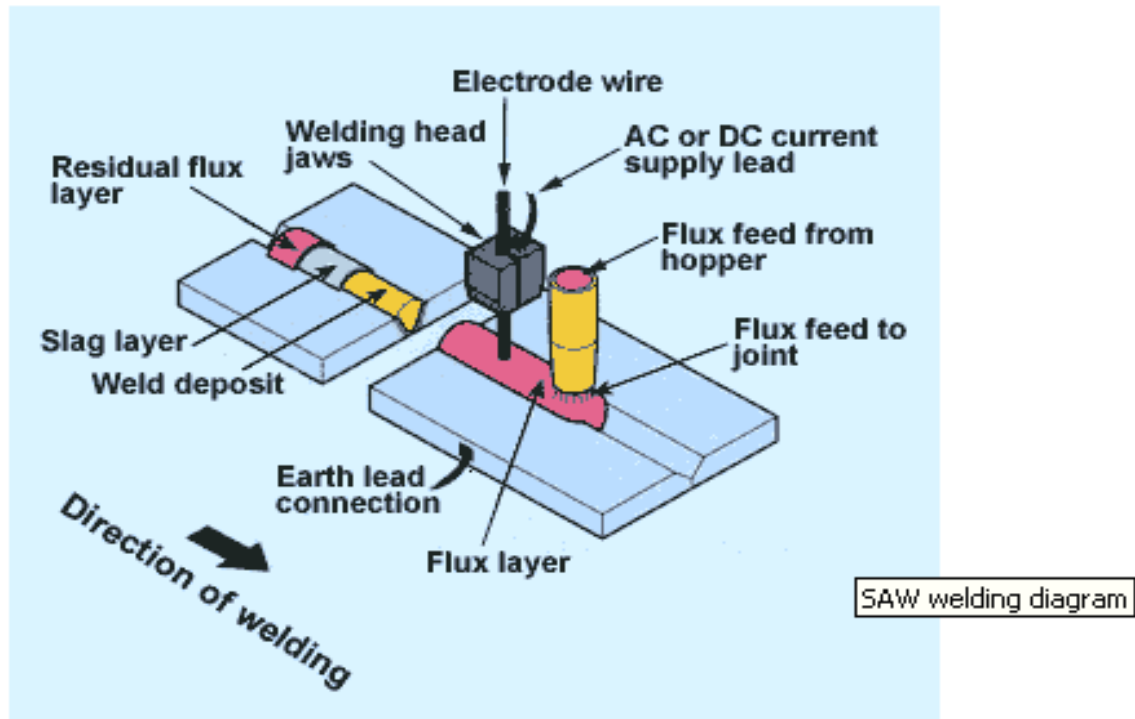


Fig. schematic diagram of SAW process

The first patent on the submerged-arc welding (SAW) process was taken out in 1935 and covered an electric arc beneath a bed of granulated flux. Developed by the E O Paton Electric Welding Institute, Russia, during the Second World War, SAW's most famous application was on the T34 tank.

Submerged Arc Welding (SAW) is a common arc (Fastening two pieces of metal together by softening with heat and applying pressure) [welding](#) process. It requires a continuously fed consumable solid or tubular (metal cored) electrode.

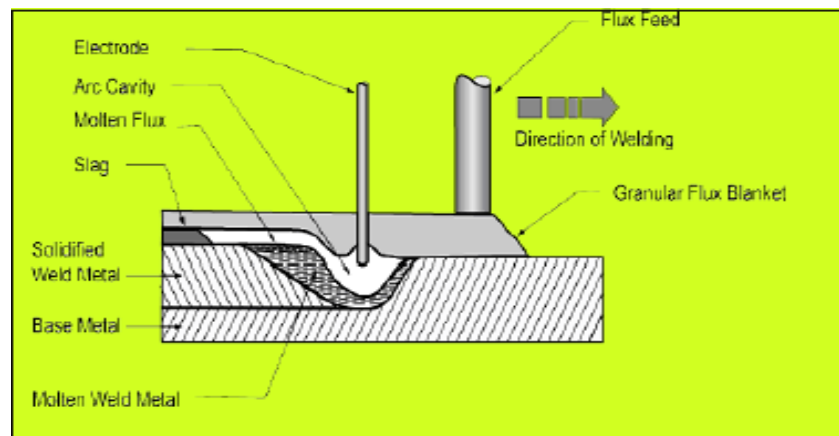


Fig. Sectional view of saw process

The molten weld and the arc zone are protected from atmospheric contamination by being “submerged” under a blanket of granular fusible (The rate of flow of energy or particles across a given surface) [flux](#). When molten, the flux becomes conductive, and provides a current path between the electrode and the work. SAW is normally operated in the automatic or mechanized mode, however, semi-automatic (hand-held) SAW guns with pressurized or gravity flux feed delivery are available. The process is normally limited to the 1F, 1G, or the 2F positions (although 2G position welds have been done with a special arrangement to support the flux). Deposition rates approaching 100 lb/h (45 kg/h) have been reported — this compares to ~10 lb/h (5 kg/h) (max) for and facts about shielded [shielded metal arc welding](#). (A steady flow (usually from natural causes)) [Currents](#) ranging from 200 to 1500 A are commonly used; currents of up to 5000 A have been used (multiple arcs). Single or multiple (2 to 5) electrode wire variations of the process exist SAW strip-cladding utilizes a flat strip electrode (e.g. 60 mm wide x 0.5 mm thick). DC or AC power can be utilized, and combinations of DC and AC are common on multiple

electrode systems. Constant Voltage [welding power supplies](#) are most commonly used, however Constant Current systems in combination with a voltage sensing wire-feeder are available.

The potential advantages of mechanized welding, several attempts were made to mechanized the arc welding process developing a continuous coated electrode as an extension of manual metal arc welding electrode was ruled out for the following reason:

- Since the Coating is non-conducting, arranging electrical contact with the electrode is not practicable.
- The coating is likely to peel off when the electrode is coiled.
- The coating is also likely to get crushed when fed through the feed rolls

Since the introduction of SAW in 1935 there has been a continuing interest in the increase of productivity without deterioration in weld quality. In submerged arc welding the weld deposit quality is welding current is determined by the type of flux, grade of wire used and following parameters

- Arc voltage
- Travel speed
- Electrode stick-out
- Heat input rate
- Size of electrode

To get optimum result one must know the effect of above parameters on bead shape, how to select them and control then properly. Series of investigation have been carried out to establish the penetrating capability of various welding processes at various

welding parameters in order to help the designers of weld men as well as welding engineers for the execution on the shop floor.

1.2 PROCESS:



Fig. photograph of welding operation

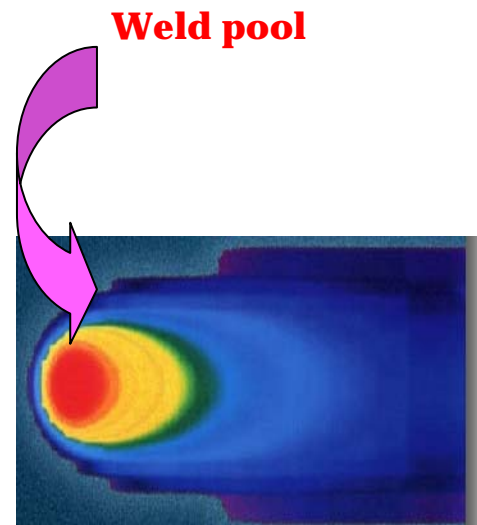


Fig. Temperature variation
electrode travel.

SAW produces coalescence of metals by heating them in arc maintained between a bare metal electrode and work piece. The arc is shielded by a blanket of granular fusible flux placed over the welding area ahead of arc. The features that distinguish SAW from other arc welding process is granular flux that covers the weld bead. SAW has been recognized for its versatility and excellent economics. It has higher metal deposition rate. It operates well at low costs, using single and multiple electrodes on plates from thin to large layers thickness. The process is most suitable for mechanization and is used for welding thick plates in long linear as arc encountered in ships, bridges, structural work, large diameter welded pipes, pressure vessels, boiler etc. The joint

produced are of very high quality. There are generally two methods by which the process can be applied. They are semi-automatic or fully automatic. In fully automatic welding, this flux is fed mechanically to the joint ahead of the arc, the wire is feed automatically to the joint ahead of the arc. In semi automatic welding, the wire feed and arc length control are automatic, while the welder moves the welding gun usually equipped with a flux-feeding device along the joint at a controlled rate of travel. Flux feed may be gravity flow, through a concentric nozzle connected to air pressurized tank, flux may also be applied in advance of welding operation or a head of the arc from a hopper run along the joint.

Submerged arc welding (SAW) is a high quality, very high deposition rate welding process. Submerged arc welding is a high deposition rate welding process commonly used to join plate.

Common Submerged Arc Welding Concerns:

We can help optimize our welding process variables. Evaluate our current welding parameters and techniques. Help eliminate common welding problems and discontinuities such as those listed below:

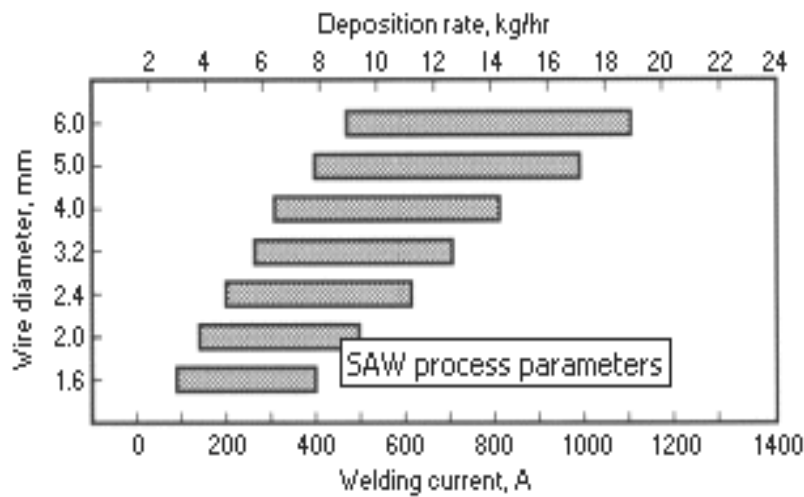
Weld Discontinuities:

- Cracks
- Porosity
- Slag
- Undercut

Submerged Arc Welding Problems:

- Solidification Cracking
- Hydrogen Cracking
- Incomplete fusion
- Irregular wire feed
- Porosity

Process features:



Similar to MIG welding, SAW involves formation of an arc between a continuously-fed bare wire electrode and the workpiece. The process uses a flux to generate protective gases and slag, and to add alloying elements to the weld pool. A shielding gas is not

required. Prior to welding, a thin layer of flux powder is placed on the workpiece surface. The arc moves along the joint line and as it does so, excess flux is recycled via a hopper. Remaining fused slag layers can be easily removed after welding. As the arc is completely covered by the flux layer, heat loss is extremely low. This produces a thermal efficiency as high as 60% (compared with 25% for manual metal arc). There is no visible arc light, welding is spatter-free and there is no need for fume extraction.

Operating characteristics:

SAW is usually operated as a fully-mechanized or automatic process, but it can be semi-automatic. Welding parameters: current, arc voltage and travel speed all affect bead shape, depth of penetration and chemical composition of the deposited weld metal. Because the operator cannot see the weld pool, greater reliance must be placed on parameter settings.

Process variants:

According to material thickness, joint type and size of component, varying the following can increase deposition rate and improve bead shape.

Wire:

SAW is normally operated with a single wire on either AC or DC current. Common variants are:

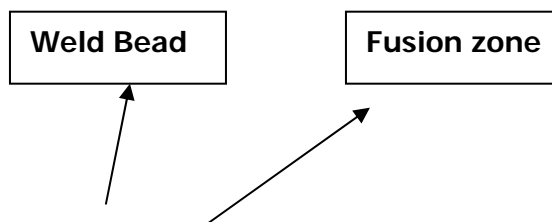
- twin wire
- triple wire
- single wire with hot wire addition
- metal powder addition

All contribute to improved productivity through a marked increase in weld metal deposition rates and/or travel speeds.

Other factors:

- Flux depth/width;
- Flux and electrode classification and type;
- Electrode wire diameter;
- Multiple electrode configurations.

1.2.1 Nomenclature of Weld bead:



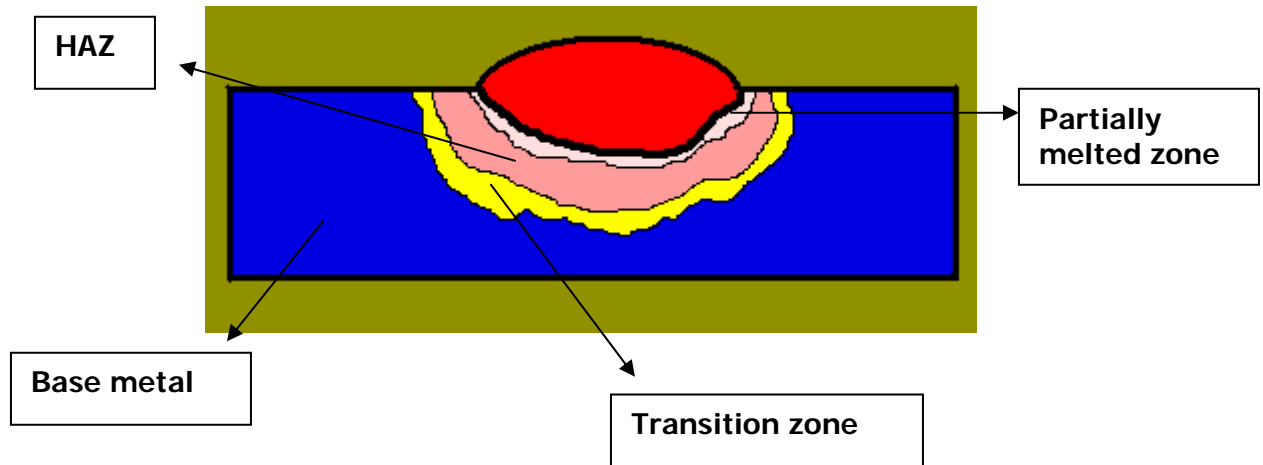


Figure of weld nomenclature.

1.3 SAW FLUXES

Fluxes used in SAW are granular fusible minerals containing oxides of manganese, silicon, titanium, aluminium, calcium, zirconium, magnesium and other compounds such as calcium fluoride. The flux is specially formulated to be compatible with a given electrode wire type so that the combination of flux and wire yields desired mechanical properties. All fluxes react with the weld pool to produce the weld metal chemical composition and mechanical properties. The flux protects the molten pool and the arc against atmospheric oxygen and nitrogen by creating an envelope of molten slag. The slag also cleans the weld metal (i.e. deoxidizes it and remove impurities such as sulphur), modifies its chemical composition and controls the profile of the weld bead. Like the manual electrode coating the SAW Flux can incorporates alloying elements. So that in combination with an unalloyed wire it will yield suitably alloyed weld metal. The molten slag also provides favorable conditions for very high current densities which, together with the insulating properties with the flux, concentrate heat into a relatively small welding zone. This results in deeply penetrating arc, which makes narrower and shallower welding grooves practicable, thus reducing the amount of weld

metal required to complete the joint. It also results in higher welding speeds. The properties of the flux enables submerged arc welds to be made over a wide range of welding currents voltage and speeds, each of which can be controlled independently of the other. Thus one can obtain welded joints of desired shapes, chemistry and mechanical properties by using an appropriate welding procedure.

The SAW flux should be so formulated so it does not evolve appreciable amount of gases under intense heat of welding zone. It should be granular in form and should be capable of flowing freely through the flux feeding tubes, valves and nozzles of standard welding equipment. Its particle size should be controlled. The flux in its solid state is a non-conductor of electricity, but when in molten condition it becomes highly conducting medium. It is therefore necessary to initiate the arc by special means. Once the arc is struck and the surrounding flux becomes molten, the welding current continues to flow across the arc, while the arc provides a conducting path of molten flux as it advances. The flux contains elements capable of assisting in the initial striking of arc and also of stabilizing it after initiation. It is common practice to refer to fluxes as 'active' if they add manganese and silicon to the weld, the amount of manganese and silicon added is influenced by the arc voltage and the welding current level. The main types of flux for SAW are:

1.3.1 CLASSIFICATION OF FLUXES :

SAW fluxes can be classified into various group as detailed:

➤ METHODS ACCORDING TO MANUFACTURING

1. Fused flux:

Ingredients are ground and mixed in a definite proportion and melted. Melting is carried out in an electric furnace, using graphite electrodes where they react chemically to form a homogeneous single mass and then they are quenched to form a metallic glass., which is crushed to the desired size sieved, sized and packed in pages or drums.

2. Agglomerated flux:

Ingredients are mixed dry and agglomerated into grains using ceramic binders at temperature in the range of 800°-900°C. This temperature of processing allows addition of metallic deoxidizers and ferro alloys, which are not possible in fused fluxes. After bonding, the mixture is dried, then crushed ground and screened into desired grain size.

3. Bounded flux:

Produced by drying the ingredients, then bonding them with a low melting point compound such as a sodium silicate. Most bonded fluxes contain metallic deoxidizers which help to prevent weld porosity. These fluxes are effective over rust and mill scale. only alkaline silicates instead of ceramic binder are used. The ingredients having alkaline silicate as binder are mixed, dry and heated up to 900°C. Metallic deoxidizers and Ferro alloys are added. After bonding mixture is dried, then crushed ground and screened into desired grain size.

➤ ACCORDING TO THE CHEMICAL NATURE:

The flux is called acidic, basic or natural depending upon the basicity index. Basicity index is defined as

$$\text{B.I.} = \frac{\text{CaO} + \text{MgO} + \text{CaF}_2 + \text{Na}_2\text{O} + \text{K}_2\text{O} + \frac{1}{2}(\text{MnO} + \text{FeO})}{\text{SiO}_2 + \frac{1}{2}(\text{Al}_2\text{O}_3 + \text{TiO}_2 + \text{ZrO}_2)}$$

The basicity index is based upon the ratio of weight of basic oxide to acidic oxides. The flux will be called as basicity index (B):

1. Acidic flux if, $B < 0.8$;
2. Neutral flux if, $B = 0.8-1.2$;
3. Basic flux if $B = 1.2-3.5$;
4. Highly Basic flux if $B > 3.5$

➤ **ACCORDING TO THE BASIC CONSTITUENTS:**

This system classifies as per their influencing constituents as given below

1. Mn-based (Mn silicate type)
2. Ca-silicate type (High, medium and low silicate type)
3. Aluminium – Rutile type
4. Aluminium – Basic type
5. Fluorides – Basic type

➤ **ACCORDING TO AWS (AMERICAN WELDING SOCIETY):**

The flux is specified by the letter F followed by a two or three digit number that indicates

the minimum tensile strength in increments of 10,000 psi. This is followed by a letter, which indicates the condition of heat treatment for testing the welds “A” stands for “as welded” and “P” stands for “post weld heat treated”. This is followed by a one or two digit number which indicates the minimum temperature in Fahrenheit of impact test to provide 20ft-lb of energy absorption (or the minimum temperature in Celsius of an impact test to provide 27 joule of energy absorption). There are eight classifications for impact strength. The classification for the flux is summarized

below: -

F	X	X	X
Flux	Mechanical Properties	Heat treatment	Minimum impact
6- (60-80,000 psi) tensile	A- as weld	20 ft- lbs@	
(48,000 psi min yield)	P-post weld	Z- no requirement	
(2% elongation in 2")	Heat-treated	0°-0°F = -18°C	
7- (70-95,000 psi) tensile		2-(-20°F) = -29°C	
(58000 psi min yield)		4-(-40°F) = -40°C	
(22% elong. In 2")		5-(-50°F) = -46°C	

8- (80-100,000 psi) tensile

6-(-60°F) = -51°C

(68,000-psi min yield)

8-(-80°F) = -62°C

(20% elong. In 2")

10-(-100°F) = -73°C

9- (90-110,000 psi) tensile

(78,000 min yield)

(17% elong. In 2")

10- (100-120,000 psi tensile)

(100,000 min yield)

1.4 OPERATING VARIABLES:

Following are the operating variables in SAW

1. Welding current
2. Arc voltage
3. Travel speed
4. Size of electrode
5. Electrode stickout
6. Plate thickness
7. Heat input rate

1.4.1. WELDING CURRENT:

It control the melting rate of the electrode and thereby the weld deposition ate.

It also control the depth of penetration. Too high a current causes excessive weld reinforcement, which is wasteful, and burn through in case of thinner plates or in

badly fitted joints, which are not proper backing. Excessive current also produces too narrow bead and undercut, excessively low current gives an unstable arc and overlapping. SAW control panel is usually provided with an ammeter to monitor and control the welding current.

1.4.2. ARC VOLTAGE:

Arc voltage means the electrical potential difference between the electrode wire tip and the surface of molten weld pool. It is indicated by the voltmeter provided on the control panel. It hardly affects the electrode melting rate, what it determines the profile and surface appearance of the weld bead. As the arc voltage increases, bead becomes wider and flatter, and the penetration decreases.

The bead width increases with an increase in arc voltage because an increase

In arc voltage provides a longer arc, which owing to its divergence is spread over

Large surface area thereby spreading the deposited metal over a wider area. The

Penetration as well as the dilution have been found to increase abruptly with the

Increase in arc voltage, what their rate of increase are found to be reduced redu-

-ced significantly with further increase of arc voltage.

► EFFECTS OF CHANGING THE VOLTAGE:

1. Increasing the voltage produces:
 - Produces wider and flatter bead
 - Increases flux consumption
 - Help to bridge the gap when fit up is poor
 - Increases pickup of alloys from flux
2. Excessively high voltages:
 - Produces hut shaped bead that is subjected to cracking
 - Produces poor slag removal in groove weld
 - Produces concave fillet weld that maybe subjected to cracking
 - Increases undercut in fillet weld
3. Low voltage:
 - Produces stiffer arc needed for getting penetration in deep grooves.
 - Resistance to arc blow.
 - An excessive low voltage produces a high, narrow bead with poor slag removal.

1.4.3 TRAVEL SPEED:

For a given combination of welding current and voltage, increase in welding speed results in lesser penetration, lesser weld reinforcement and lower heat input rate Excessively high travel speed, decreases fusion between the weld deposit and the parent metal, increases the tendencies for undercut , arc blow,

porosity and irregular bead shape. As the speed decreases, penetration and reinforcement increases but too slow a speed result in poor penetration. Excessively high welding speed decreases the wetting action and increases the probability of undercutting, arc blow, and weld porosity and uneven bead shapes. Excessively low speed also produces a convex hat shape beads that are subjected to cracking cause excessively melt through and produces a large weld puddle that flows around the arc resulting in rough bead, spatter and slag inclusions.

1.4.4 SIZE OF ELECTRODE

A given welding current changing over electrode result in wider less penetrating bead. Hence in joints with poor fit-up a large electrode is preferred to a smaller one for bridging the root gap. For a given electrode size a high current density results in a strong, penetrating arc, while a lower current density gives a soft arc which is less penetrating.

1.4.5 ELECTRODE STICKOUT:

It is also termed as electrode extension. It refers to the length of electrode between end of contact tube and the arc, which is subjected to resistance heating at the high current densities used in the process. The longer the stickout, the increase in deposition rate is accompanied by a decrease in penetration. Hence longer stick-out is avoided when deep penetration is desired.

1.4. 6 PLATE THICKNESS:

As the plate thickness increases the value of hardness of the weld and HAZ decreases slightly if the increase in plate thickness is not higher (say 3-9 mm). Since, due to the decrease of cooling rate of higher thickness plate.

1.47 HEAT INPUT RATE:

The heat input rate is directly proportional to the current and voltage and inversely proportional to the travel speed, as the formula is given by

$$\text{HIR} = \frac{V * A}{S}$$

Where HIR= heat input rate in j/mm

V = Arc voltage

A= welding current (amp)

S= Arc travel speed in mm/sec

For a given joint thickness, higher the heat input rate the lower is the cooling rate of the weld metal and heat affected zone of parent metal and vice versa. Heat input rate has an important bearing on the weld metal microstructure and the final microstructure of haz and thereby on the toughness.

1.5 Submerged Arc Welding Benefits:

- Extremely high deposition rates possible (over 100 lb/h (45 kg/h);
- Sound welds are readily made (with good process design and control);
- Deep weld penetration;
- High speed welding of thin sheet steels at over 100 in/min (2.5 m/min) is possible;
- Easily automated;
- Minimal welding fume or arc light is emitted;
- Low operator skill required.

1.6 Limitations of SAW

- Limited to ferrous (steel or stainless steels) and some nickel based alloys;
- Normally limited to the 1F, 1G, and 2F positions;
- Normally limited to long straight seams or rotated pipes or vessels;
- Requires relatively troublesome flux handling systems;
- Flux and slag residue can present a health & safety issue;
- Requires inter-pass and post weld slag removal.

1.7 Applications:

SAW is ideally suited for longitudinal and circumferential butt and fillet welds. However, because of high fluidity of the weld pool, molten slag and loose flux layer, welding is generally carried out on butt joints in the flat position and fillet joints in both the flat and horizontal-vertical positions. For circumferential joints, the workpiece is rotated under a fixed welding head with welding taking place in the flat position. Depending on material thickness, either single-pass, two-pass or multipass weld procedures can be carried out. There is virtually no restriction on the material thickness, provided a suitable joint preparation is adopted. Most commonly welded materials are carbon-manganese steels, low alloy steels and stainless steels, although the process is capable of welding some non-ferrous materials with judicious choice of electrode filler wire and flux combinations.

Major application in industry:

- Used in manufacturing of ship and heavy structural parts.
- Nowadays it is widely used in repairing of machine parts by depositing cladding and hardfacing.
- Fabrication of pipes, penstocks, pressure vessels, boiler, railroad, structure of railway coaches and locomotive.
- Automotive, Aviation and nuclear industry.
- For welding mild steel, medium & high tensile low alloy steels.

Properties of the weld metal:

properties of the weld metal are toughness and strength. In general the strength and toughness of the weld metal do not match those of corresponding base metal. Therefore if equal strength is required of the weld metal and the base metal in a weldment then the yield stress of weld metal will have to be higher because with an equal yield stress, strength of the weld will be lower. Properties of weld metals are greatly influenced by the type of microstructure, grain size, as also by precipitation process etc. And microstructure can be affected considerably by welding parameters like welding speed, heat input etc. Thus it is important to know the effect of microstructure and grain size on hardness of the weld.

1.8 Weld metal microconstituents:

The two basic constituents of steel obtained on slow cooling to room temperature are ferrite and cementite.

1.9.1 Ferrite, or α -iron is almost pure iron but carbon can be dissolved on it to form a solid solution ferrite which can contain upto 0.0006% C at room temperature and that can increase to 0.05% at 750°C. But ferrite is capable of dissolving a large number of second elements other than carbon to form α solid-solution. Heating and fusion influence the size of these grains. Ferrite is soft, weak and ductile.

1.9.2 Cementite is a chemical compound of iron and carbon which contains 6.67% carbon and is formed around 1500°C. It is the hardest constituent found in iron-carbon alloys. Cementite can dissolve a wide variety of elements such as Mn and Cr, to give complex carbides. Cementite is hard and brittle. Cementite can be present as free or laminated with ferrite to produce a structure called Pearlite. Primary cementite solidifies directly from melt and occurs in the form of hard regions or needles (white iron), while it outlines the grain structure in hypereutectoid steel. Secondary cementite precipitates in solid, at low carbon contents, at lower critical temperature (A_1) and it occurs along the ferrite grain boundaries. This type of cementite is frequently encountered in weld metal with very low carbon content.

Different microstructural phases encountered in fusion welding of steel can be grouped into three types *viz.*, the primary microstructure, the secondary microstructure and tertiary microstructure.

1.9.3 Primary microstructure is the one obtained by direct solidification of molten metal and usually results in a cast structure with columnar grains. The length of these grains is nearly parallel to the direction of the temperature gradient during solidification. Sometimes a dendrite sub-structure can be observed inside the

columnar grains. the major primary microstructural products encountered in carbon steel welds are δ -ferrite and austenite or γ -iron.

1.9.4 Secondary microstructure is the one obtained by transformation of solid phase austenite into different other solid phases like Pearlite, bainite, martensite, grain boundary ferrite, ferrite side plates, lath ferrite, acicular ferrite, polygon ferrite and retained austenite.

1.9.5 Tertiary microstructure is encountered only in multi-run welds where, due to the successive runs, the previous runs are heated to austenite region and thus result in products of different fineness affecting the mechanical strength and toughness properties due to the normalizing affect of heating by successive runs.

The following microstructure microstructures may be encountered in weld metal and HAZ of steel welds:-

1.9.a Delta ferrite- Delta ferrite nucleates from the melt if steel contains less than 0.53%C; however this phase is suitable only above 1390°C. Thus, with lowering of temperature it changes to austenite.

1.9.b Austenite- Austenite or γ -iron is stable at high temperature between 1390°C and 910°C; it crystallizes in the FCC cell structure and is thus more closely packed than the ferrite cell BCC Structure. The cast austenite structure in the weld metal zone is usually regarded as the primary microstructure which is maintained

during cooling until the γ - α transition temperature is reached. Austenite is non magnetic and relatively weak. In slowly cooled steels it cannot exist at temperatures below 695°C and is fully decomposed when temperature of a plain carbon steels falls below that temperature.

1.9.c Grain boundary ferrite (GBF) - During cooling of the weldment, on reaching the γ - α transition stage, one of the secondary transformation products is grain boundary ferrite, which marks the original austenite grain. The primary microstructure therefore remains recognizable in as deposited weld metal, particularly at moderate magnification of up to 100x. Grain boundary ferrite is often referred to as pro-eutectoid ferrite.

GBF is normally considered detrimental to toughness, because of its coarse grain structure, compared with acicular ferrite. it has been reported that cracks in ferritic weld metal is normally propagate along GBF, a process which is intensified by the presence of brittle pearlitic structures along grain boundaries . GBF is also sometimes called blocky ferrite.

1.9.d Ferrites side plates- In a cross sectional view ferrites side plates appears as long needles with aspects ratio (length/width) of at least 20:1. This microstructural constituent grows from grain boundary ferrite into the original austenite grain as packets of parallel plates. Ferrites side plates, like grain boundary

ferrites, are also detrimental to toughness. This is link with the possible presence of precipitated carbides, retained austenite and martensite by low angle grain boundaries, causing a much larger effective grain size.

1.9.e Lath Ferrite - It is an intra granular (i.e. within grains) austenite transformation product resembling lower bainite. It is found amongst acicular ferrite or side plate structures. Unlike ferrite side plates; lath ferrite is not attached to grain boundary ferrite. Lath ferrite is also detrimental to toughness on the similar consideration as the ferrite side plate.

1.9.f Polygonal ferrite- It occurs in the form of coarse ferrite island inside the prior austenite grain .Polygonal ferrite like grain boundary is detrimental to toughness because of its coarse grain size.

1.9.g Acicular ferrite- It is formed in the interior of the original austenite grains by direct nucleation from the inclusion resulting in the randomly oriented short ferrite needles with a basket weave feature .for the various advantages of acicular ferrite microstructure it is aimed to increase its presence in the weld metal. It is found that composition control of the weld metal is necessary in order to maximize the volume fraction of acicular ferrite, because excessive allowing elements can cause the formation of bainite and martensite.

1.9.h Pearlite- A microstructure formed with alternate lamellar layers of cementite and ferrite is called as Pearlite. It is so named because when etched and viewed with naked eye, it has the appearance of “mother of pearl”. Pearlite combines good properties of ferrite and cementite. Pearlite grain size is defined by the distance between the cementite lamellae, which varies with the heat treatment conditions.

Pearlite adversely influences the toughness of ferritic weld metal, particularly when brittle cementite lamellae are lying in the crack direction. Reduction of inter-lamellar spacing is detrimental, whereas decrease in thickness of cementite lamellae is beneficial to toughness because thinner carbides are more likely to deform than to crack upon stress.

1.9.i Bainite- Depending upon cooling rate austenite may transform into Pearlite, bainite or martensite the intermediate transformation with fast and very fast cooling rate, results in the formation of structure called bainite. While fast cooling rate is said to give coarse or upper bainite, very fast cooling rate results in fine or lower bainite. Lower bainite consists of ferrite and containing small carbide grains align parallel to each other and at 60 deg. to the ferrite axis. Upper bainite consists of ferrite containing carbides aligned along with ferrite axis.

1.9.j Martensite and retained Austenite- If the steel is quenched from the austenite conditions, the excess carbon will be trapped within the lattice to form the

supersaturated solid solution of carbon in α -iron called martensite. martensite is a fine, niddle like structure, which, due to the enormous super saturation that causes the distortion of the cubic lattice, is very strong and hard, but very brittle. Martensite s the hardest constituent of the steel. it is however mainly due to the distortion of the tetragonal lattice, which increases with the increases in carbon.

1.10 Types of grain exists in weldments

- a) **Fine grain-** This kind of grain exists in the HAZ area due to recrystallization of the base metal. The hradness of the fine grain is more then that of coarser grain.
- b) **Coarse grain-** Coarse or columnar grains are formed in the weld zone due to formation of primary microstructure that cools directionally along temperature gradient.
- c) **Medium size grain-** The base metal grain size is usually said as medium size grain as compare to columnar weld metal grain.
- d) **Fine grain in the matrix of medium size grain-** This kind of grain are generally found in the Transition zone of HAZ due to partial refinement of the grain of base metal.

1.9 **Objective of present work:**

The aim of the present work is to study the effect of heat-input on microstructure and grain size of bead on plate weld at various parameters.

Since the mechanical properties is directly related to the microstructure and grains.

So the study in this area can improve the mechanical properties of the weldments.

2. EXPERIMENTATION:

2.1 Welding Equipment

Machine used in Welding Laboratory, Delhi College of Engineering, Delhi.

Manufacture by: -- Quality Engineer (Baroda Pvt. Ltd.), A/18, Gujarat Estate,

Dharamsingh Desai Marg, Chhani Road Baroda -390002

M/c Model: -- QSW800

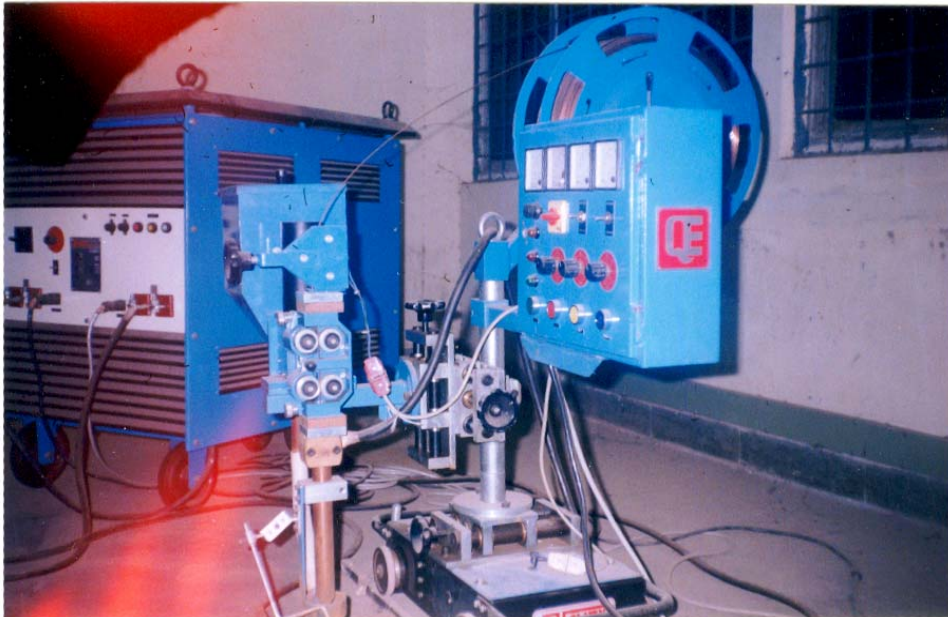


Fig. 5. Picture of SAW machine used for Experimental work

Supply voltage: -- 380/440

Phase Three

Frequency: -- 50 Hz

Range of Welding: -- 800 Amp.

O.C.V. Of Rectifier: -- 10-52 Volts

Maximum Welding Current at 100% duty cycle: -- 900 Amp

Operating voltage: -- 26- 60 Volts

2.2 Base Metal

For carrying out proposed work , test specimen were prepared from 12 mm thickness Mild steel plate. Dimension of each plate were 200*65*12mm. composition of the base material as supplied by the supplier was as follows:

C	S	Mn	S
0.19%	0.015%	1.72%	0.3%

2.3 Consumables:

2.3.1 Filler Wire:

2.5 mm diameter copper coated mild steel wire manufactured by (ESAB INDA LTD) was used specification of filler wire used was (AWS-A5.17 EL-8).

The chemical composition of filler wire was:

C	Mn	Si
0.10%	0.45%	0.02%

2.3.2 Flux:

The study was carried out by using available flux i.e. an agglomerated Flux

Manufactured by ESAB INDIA LTD.

The specification of the flux was:

Automelt Gr.II, Coding - AWS / SFA 5.17

F7AZ - EL8

F7PZ - EL8

The Chemical Composition was:

C	Mn	Sn
0.08%	1.00%	0.25%

2.4. WorkStation used for Image analysis consisting:

CCD camera, Optical Microscope and Video Monitor attached to the computer.

2.5 Software used:

GAIA BLUE MATERIAL 5.3

2.51 Some introduction of the features of the software that were used:

The following features were used for Phase analysis:

2.5.1.1 Common Processing of Histogram window:

The histogram window displays cumulative distribution graph of intensity. This support binarization function. The histogram window has the type of single binarization and multiple binarization.

2.5.1.1.a Single Binarization:

This divides two parts as interest area and background area. This is used dialog box of graphite, hardness, and thickness.

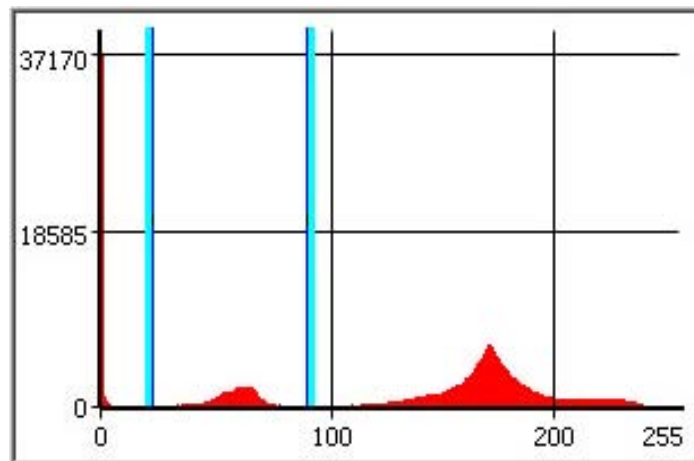


Fig 2.5.1.1.a Showing the single Binarization

Interested area: Area of intensity between lower bar and higher bar.

Background area- Area of intensity except interested area.

X: Intensity of image (0~255)

Y: Cumulative value of intensity (0~all the number of pixel composed image).

Bar-This displayed vertical line colored cyan in Figure 2.5.1.a this can adjust by mouse dragging.

Lower bar: This bar located left in figure 2.5.1.a adjusts lower threshold value.

Higher bar: this bar located right in figure 2.5.1.a adjusts higher threshold value.

2.5.1.1.b Multiple binarization:

This divides part of interested area from one up and background area. This is used dialog box of phase. This has same function of single binarization except existence of interested area from one up. This is represented by various colors in figure 2.5.1.1.b

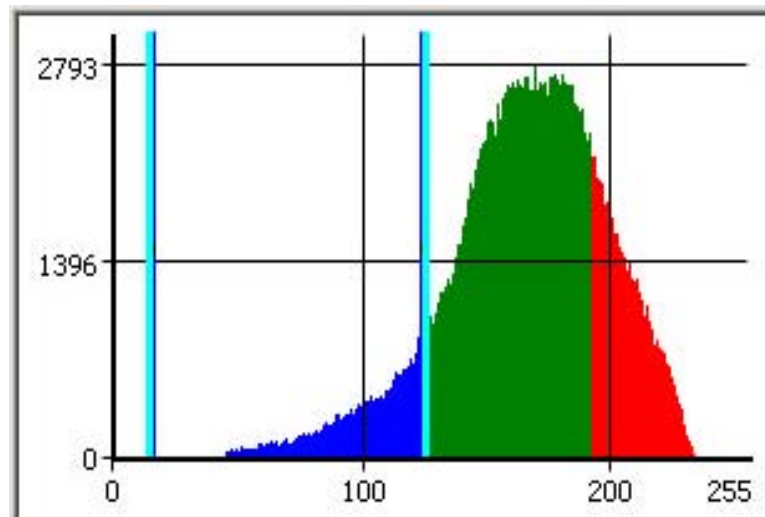


Figure 2.5.1.1.b of multiple binarization

2.5.1.2 The following features were used for grain analysis:

Components –

File Name: Display File Name of image. .

Result Table: Display analysis data.

Field Area: Field area of image.

Total Number: Total number of grains detected.

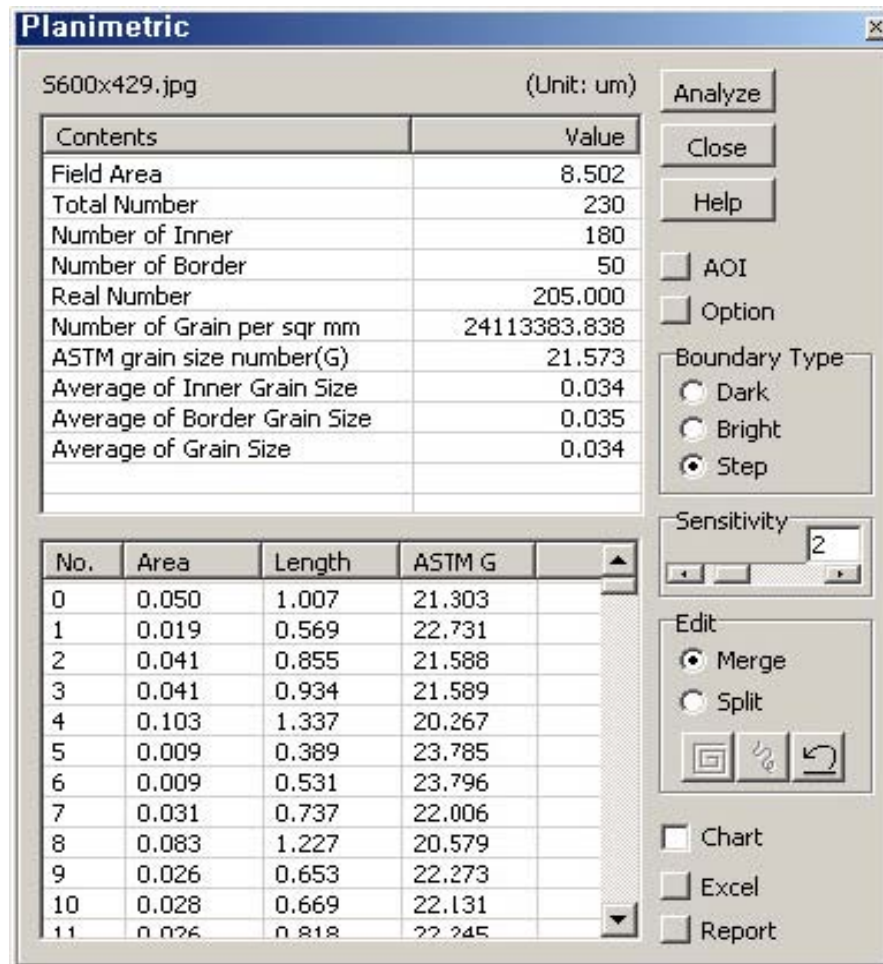


Figure of the result of the Grain size analysis

Number of Inner: The number of inner grains, which do not adhere with border.

Number of Border: The number of outer grains which adhere with border.

Real Number: The number of grains to calculate number of grain per sqr. mm.

Number of Grain per sqr mm :

NA = the number of grains which exist in 1 square millimeter
area

ASTM grain size number(G) : Average grain size based on

ASTME112.

The equation is followed

$$G = \frac{\log NA}{\log 2} - 2.95$$

Average of Inner Grain Size: Average of inner grain size based on real area in second column of grain table.

Average of Border Grain Size: Average of outer grain size based on real area in second column of grain table.

Average of Grain Size: Average of total grain size based on real area in second column of grain table.

Measure Table Display each individual data of grains detected in image. When click a item in table, the appropriate grain is displayed in image.

No.: Unique identification number of individual grain.

Area: Area of individual grain.

Length: Length of individual grain.

ASTM G: Individual grain size based on ASTM E112.

Boundary Type Determine Boundary Type of grain in original image

- ☒ Dark: Boundary is dark and face is bright.
- ☒ Bright: Boundary is bright and face is dark.
- ☒ Step: Each gray value of grain face is more than 2, or boundary is ambiguous.

Sensitivity: Determine coarseness of grain. When Sensitivity is closer to 1, grain is coarser. On the contrary, When Sensitivity is closer to 10, grain is finer.

Edit Merge and split of grain in image.

☒ Merge: To select two grain, click left mouse button on active window. And then when click right mouse button, two grains merge into one grain.

☒ Split: Determine type of split line. Select a grain to split using left mouse button and then draw split line. When click right mouse button, one grain split into two grain.

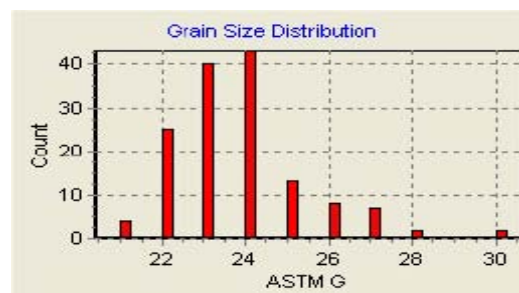
☒ Type of Split line:

☐ (Poly-line): Create poly-line by connecting the clicked points on the image.

☐ (Free-draw line): It draws a free line.

Analyze When this button clicked, the measure of grain size is operated. The result is displayed on result table and measure table. This operation requires long time.

Chart If select chart, display graph that calculated cumulative distribution of ASTM G of grain table --



2.6 The Research work was carried out in the following steps:

- The experiments were carried out with different value of Current, Voltage and Travel speed.

- The Prepared Weld samples were polished and etched.
- And then the samples were tested for Hardness.
- Lastly the Specimen's microstructure Photograph were analyzed for Phases & grain size.
- The resulted data were compared and analyzed for conclusion.

2.7 EXPERIMENTAL PROCEDURE

The experiment has been performed on constant voltage fully automatic submerged arc welding machine of 800 A, 380/440/3-phase .50 H z rectifier type power source, 3.2mm copper coated mild steel electrode Varying the parameters carried out bead on plate test. After welding samples were prepared for various current, voltage and travel speed parameters (Table 1-3). The various samples were prepared by dry polishing the surface of specimens with various grades of polish papers of silicon carbide (water-proof), starting with 220, 320, 400 and 600. After this the specimens were polished on rotating disc with paste of alumina (Al_2O_3) abrasive powder (fine size of 6um), water were used as coolants. Finally the specimens were etched by 2% nital (Containing 98 cm³ ethanol and 2 cm³ nitric acid) and then washed off with water. Then the specimens were dried by means of blower and the microstructure of specimen was recorded by means of metallurgical microscope attached with CCD camera. Then the specimens were tested

under Optical Brinell hardness machine under the load of 750 kg to find the hardness for weld, Heat affected Zones (HAZ 1, HAZ 2, and HAZ 3) is shown in tables. The picture of microstructure of the specimens was analyzed by using the software GAIA BLUE, GAIA MATERIAL/ ONIX Metallurgy Plus and the data were collected and the graphs were drawn accordingly.

3. RESULTS & DISCUSSIONS:

Influence of increasing the Heat-input on microstructure, grain size and thus on hardness:

Since Heat-input can be increased by increasing the current and voltage and also by reducing the travel speed, here we were taken two parameter current and voltage as to increase the Heat-input and tried to find some conclusions.

3.1 Effect of increasing welding current

Voltage constant = 38 volts

Starting current = 510 amp, Constant Travel speed = 14.3 mm/s

Sl. No.	Voltage (volts)	Current (amps)	Wire Feed (mm/s)	Travel Speed (mm/s)	HIR (j/mm)	Weld Brnll. Hardness	HAZ1 Brnll. Hrd.	HAZ2 Brnll. Hrd.	HAZ3 Brnll. Hrd.	Base-Metal Hrd.
1	38	510	79.6	14.3	1355.5	285	258	249	241	160
2	38	550	91.5	14.3	1461.5	321	281	260	249	160
3	38	600	100	14.3	1594.4	361	297	274	270	160

Table 1. Here voltage and travel speed were taken as constant and wire feed i.e. current was increased.

3.1.1 Effect of increasing welding current on phases

The following are the images of phase analysis --

Phase analysis of fusion zone:

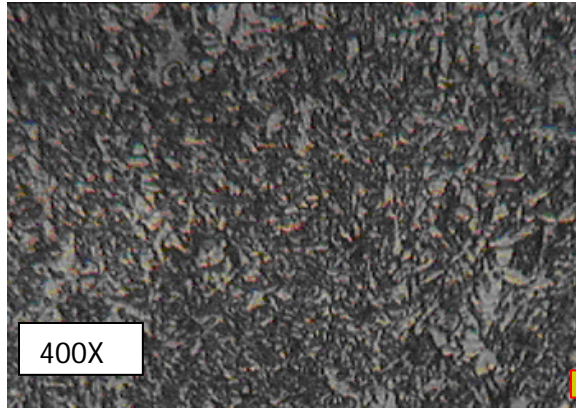


Fig. 6 Microstructure of fusion zone of sl no.1

(Current=510 amp, Voltage=38 volt, Travel Speed= 14.3mm/s)

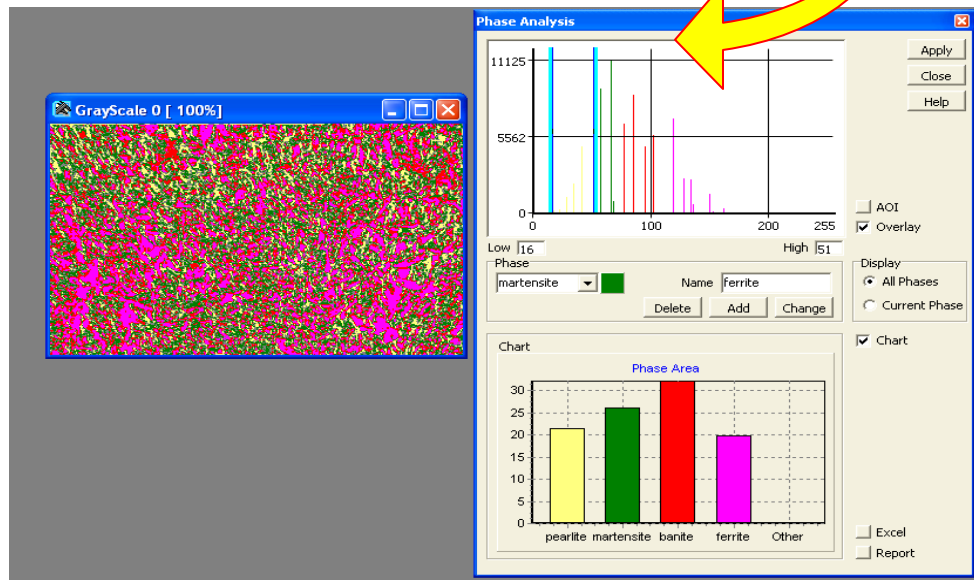


Fig. 7 Result of Phase Analysis-

(Pearlite – 22%, Martensite- 26%, Bainite – 32%, and Ferrite – 20%)

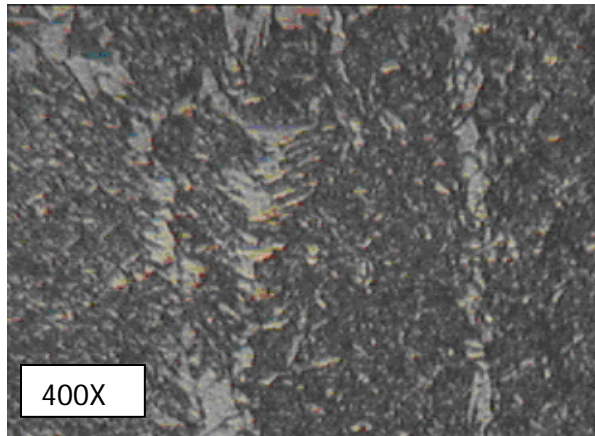


Fig. 8 Microstructure of fusion zone of Sl. No.2

(Current=550 amp, Voltage=38 volt, Travel Speed= 14.3mm/s)

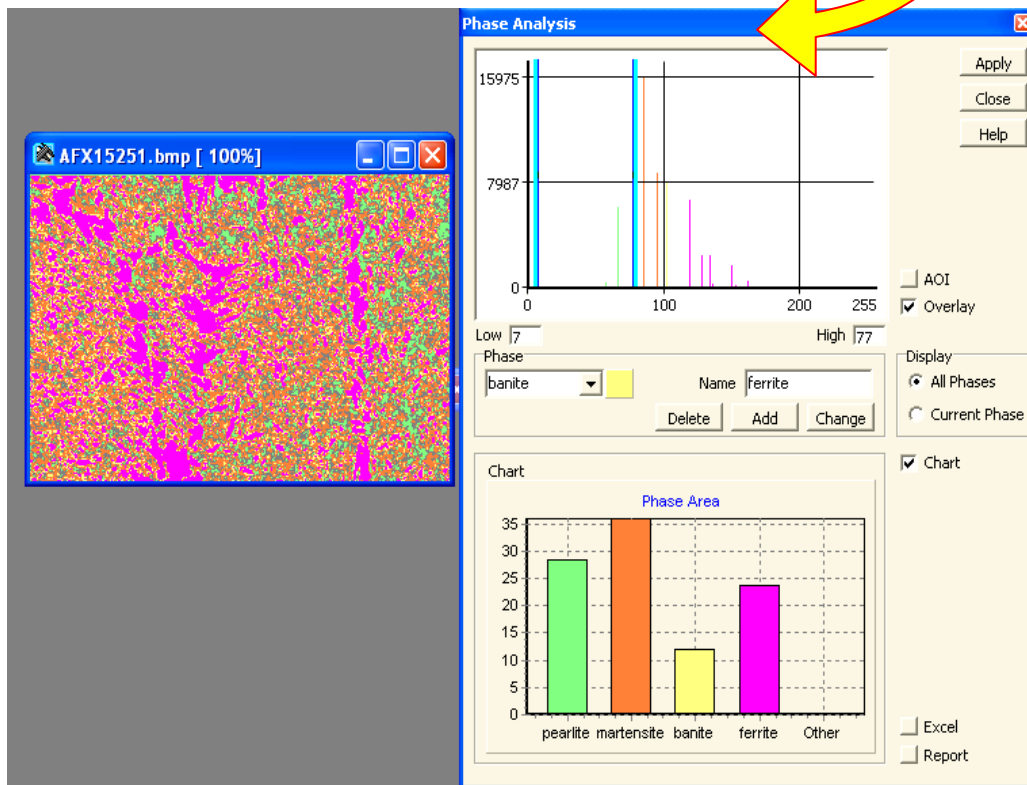


Fig. 9 Result of Phase Analysis-

(Pearlite – 29%, Martensite- 36%, Bainite – 13%, and Ferrite – 22%)

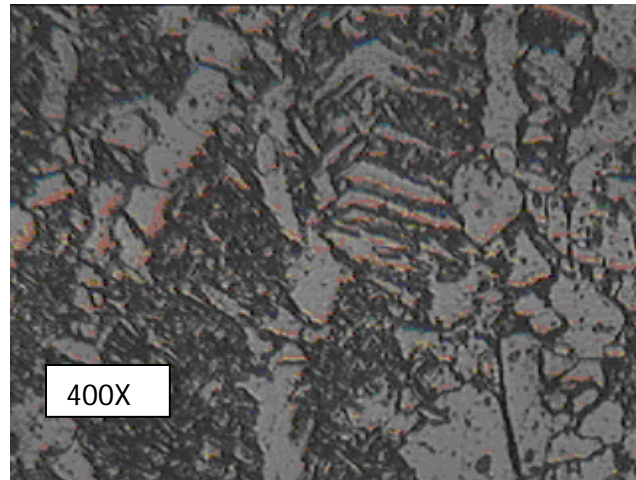


Fig. 10 Microstructure of fusion zone of Sl no. 3

(Current=600 amp, Voltage=38 volt, Travel Speed= 14.3mm/s)

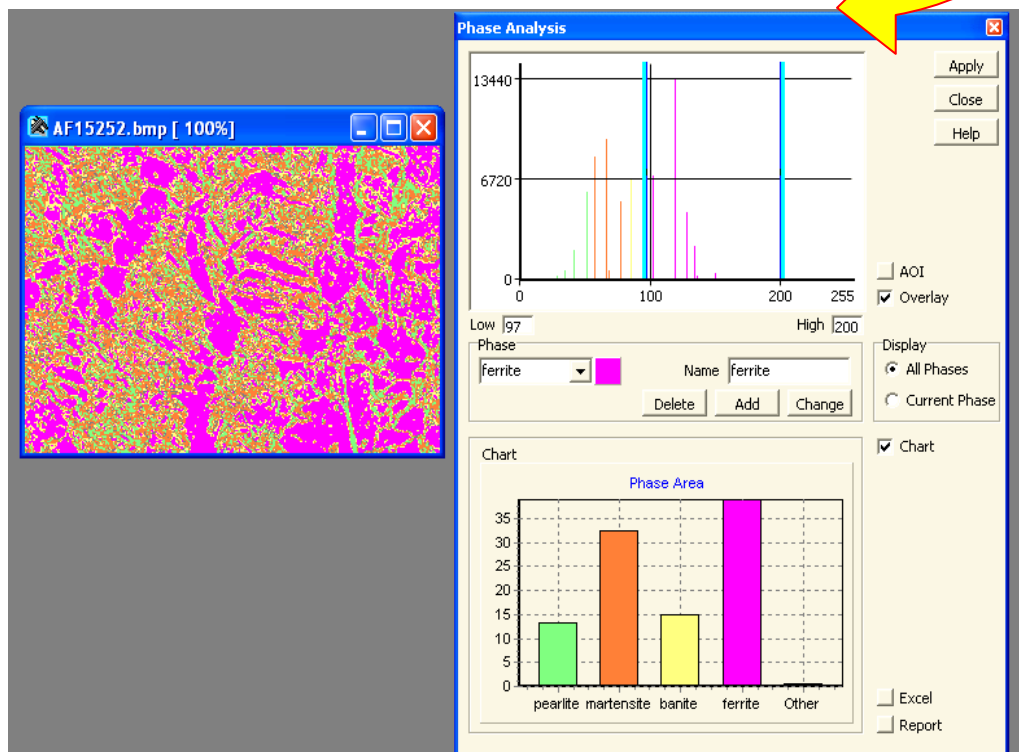
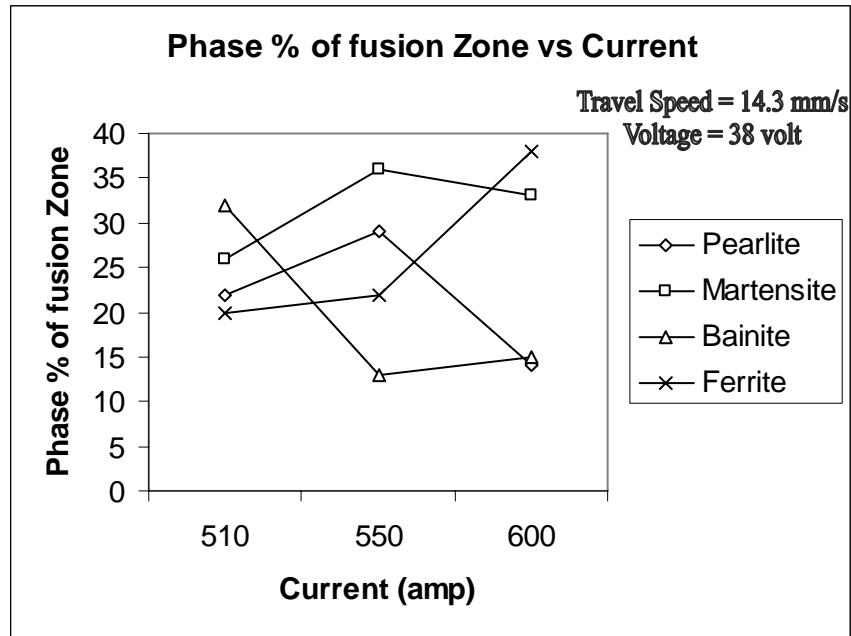


Fig.11 Result of Phase Analysis-

(Pearlite – 14%, Martensite- 33% , Bainite – 15%, and Ferrite – 38%)

The following is the resulting Graph-



Graph 1. Drawn between percentage of Phases versus current for Fusion zone

➤ **Observations:**

The resultant graph of phase analysis showing the % change in microstructure in fusion zone as the current was increased. Here we were observed in the Fusion zone that the composition of ferrite was increased as the current increased but the % of Pearlite, martenste and bainite were decreases. Since the weld bead upper surface gets high cooling as compare to the HAZ and thus the formation of martensite decreases as current increases because of high heat input (lower the cooling rate and thus objects the formation of martensite and bainite).

Phase analysis images of HAZ:

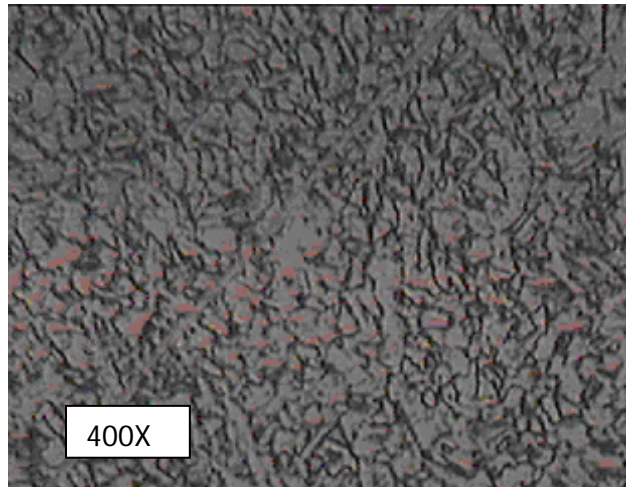


Fig. 12 Microstructure of HAZ SL of no. 1

(Current=510 amp, Voltage=38 volt, Travel Speed= 14.3mm/s)

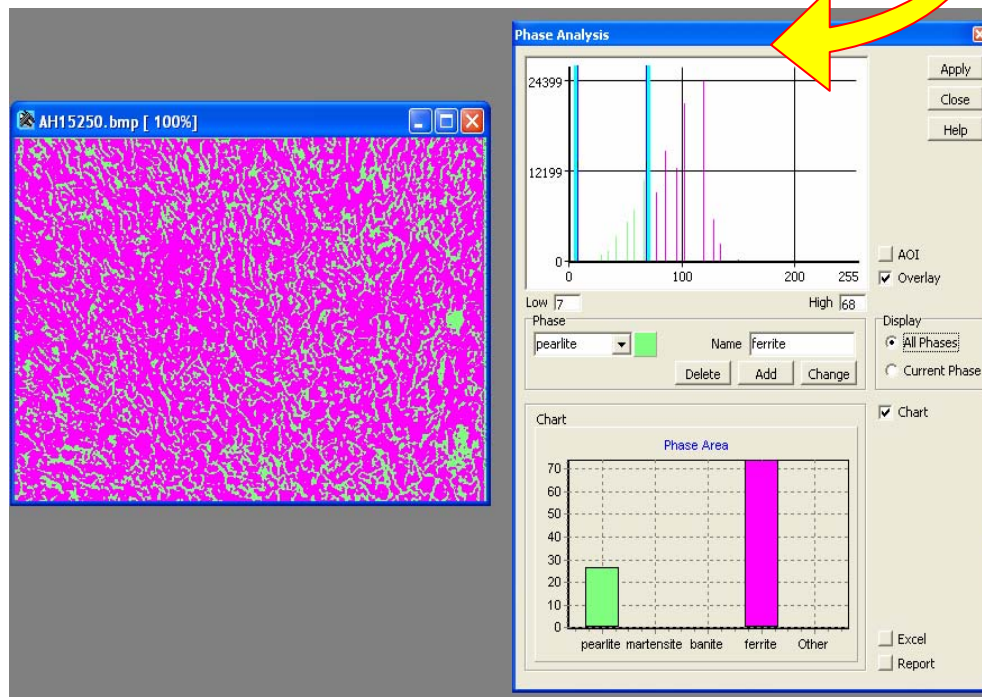


Fig.13 Result of Phase Analysis-

(Pearlite – 28%, Martensite- 0% , Bainite – 0%, and Ferrite – 72%)

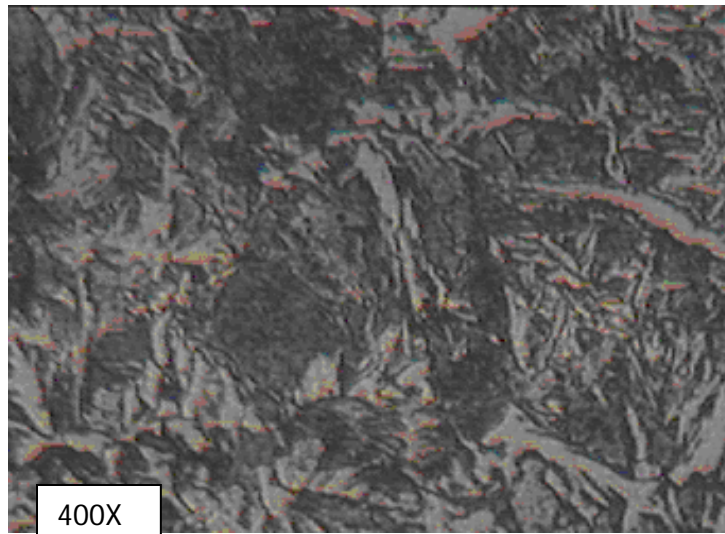


Fig. 14 Microstructure of HAZ Sl no. 2

(Current=550 amp, Voltage=38 volt, Travel Speed= 14.3mm/s)

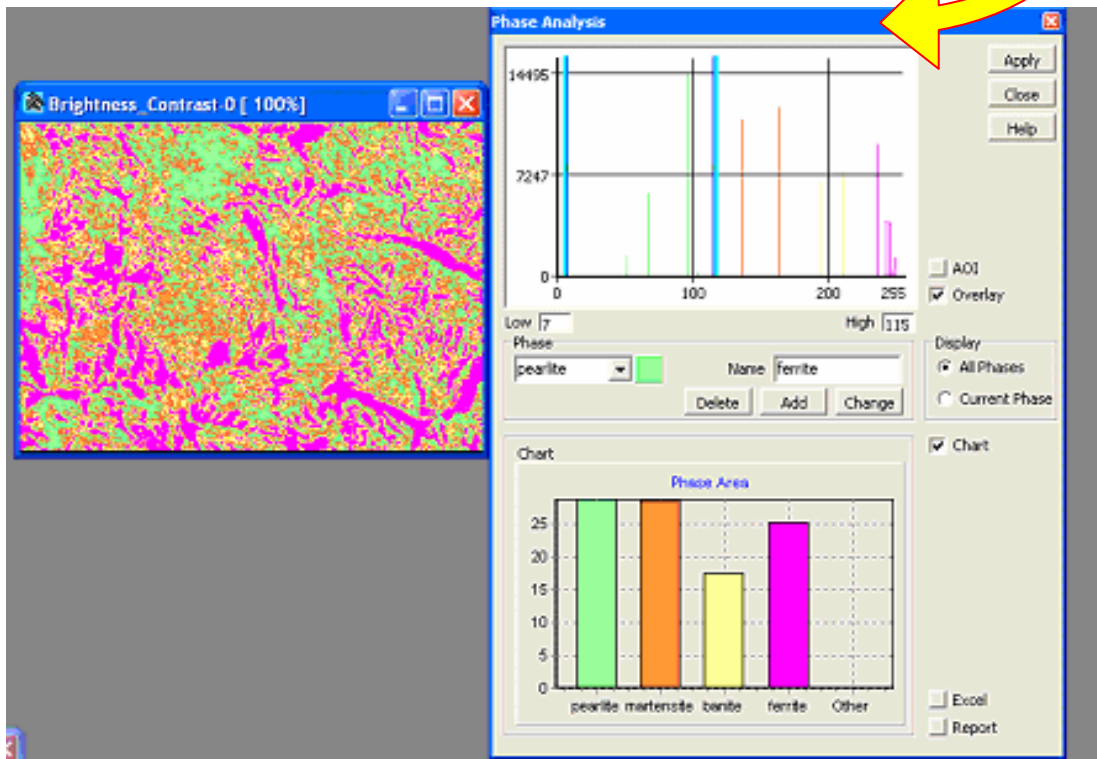


Fig.15 Result of Phase Analysis-

(Pearlite – 28%, Martensite-28%, Bainite – 18%, and Ferrite – 26%)

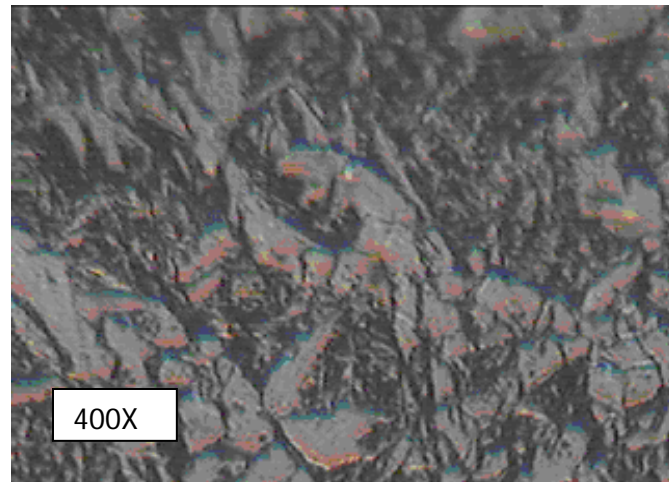


Fig. 16 Microstructure of HAZ Sl no.3

(Current=600 amp, Voltage=38 volt, Travel Speed= 14.3mm/s)

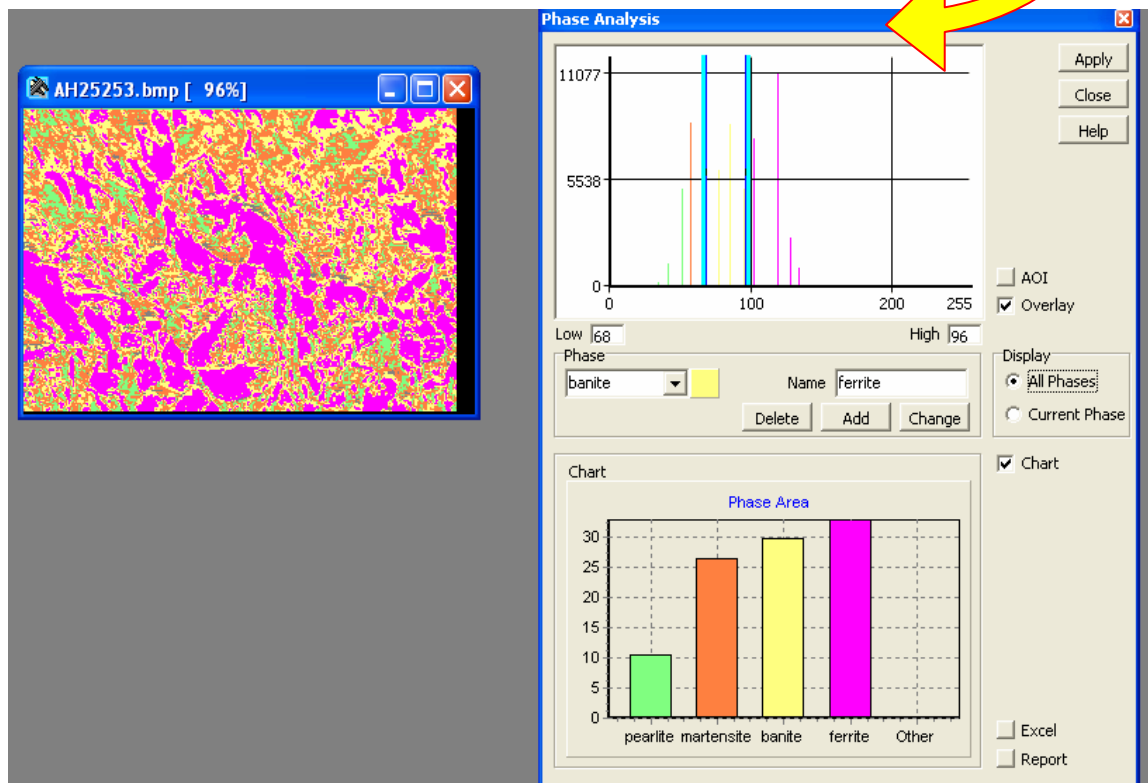
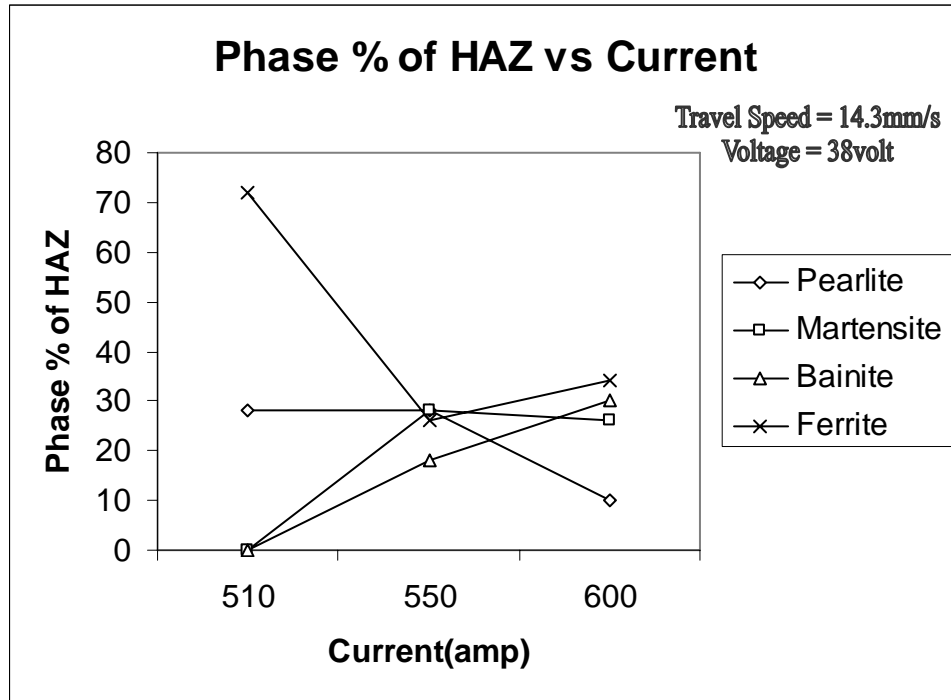


Fig.17 Result of Phase Analysis-

(Pearlite – 10%, Martensite-26%, Bainite – 30%, and Ferrite – 34%)

The following is the Resulting Graph--



Graph 2. Drawn between percentage of Phases versus current for HAZ

➤ **Observations:**

The resultant graph of phase analysis showing the % change in microstructure in HAZ as the current was increased. It is clear from the graph that as the current increase the percentage composition of martensite and ferrite decreases but Pearlite and bainite increases. The considerable changes occurred in ferrite and Pearlite.

Phase analysis images of Transition zone:

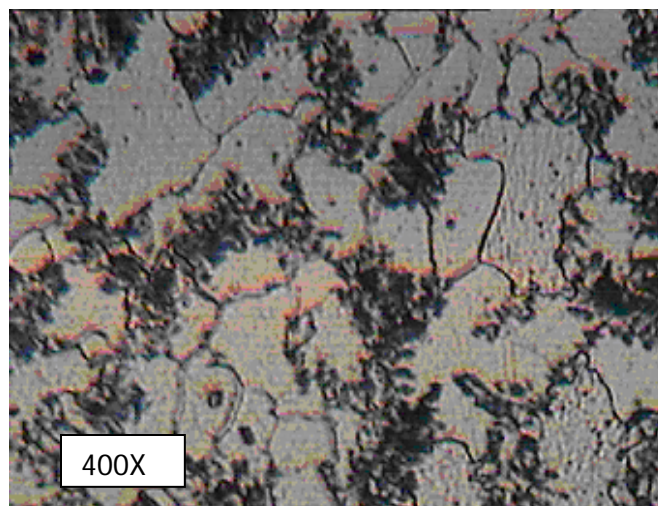


Fig. 18 Microstructure of transition zone of SL no.1

(Current=510 amp, Voltage=38 volt, Travel Speed= 14.3mm/s)

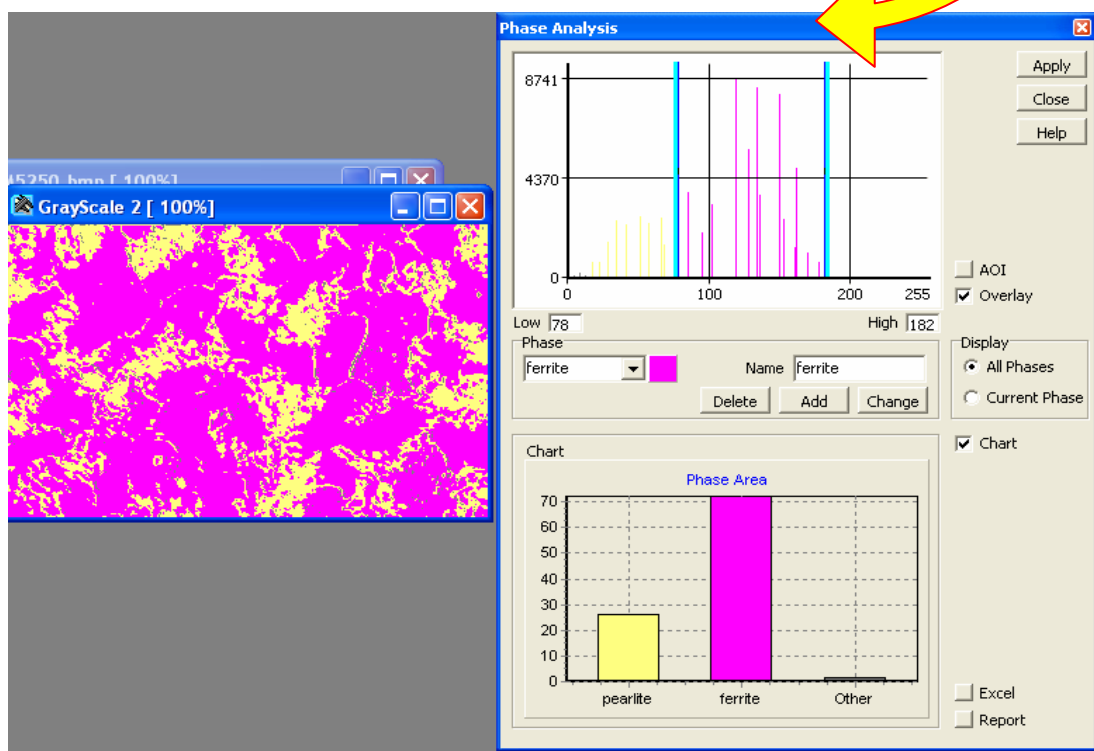


Fig.19 Result of Phase Analysis--

(Pearlite – 28 and Ferrite – 72%)

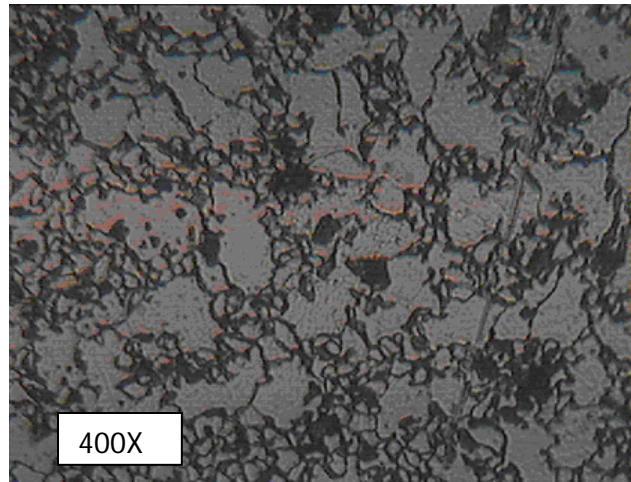


Fig. 20 Microstructure of Transition zone of sl no.2
(Current=550 amp, Voltage=38 volt, Travel Speed= 14.3mm/s)

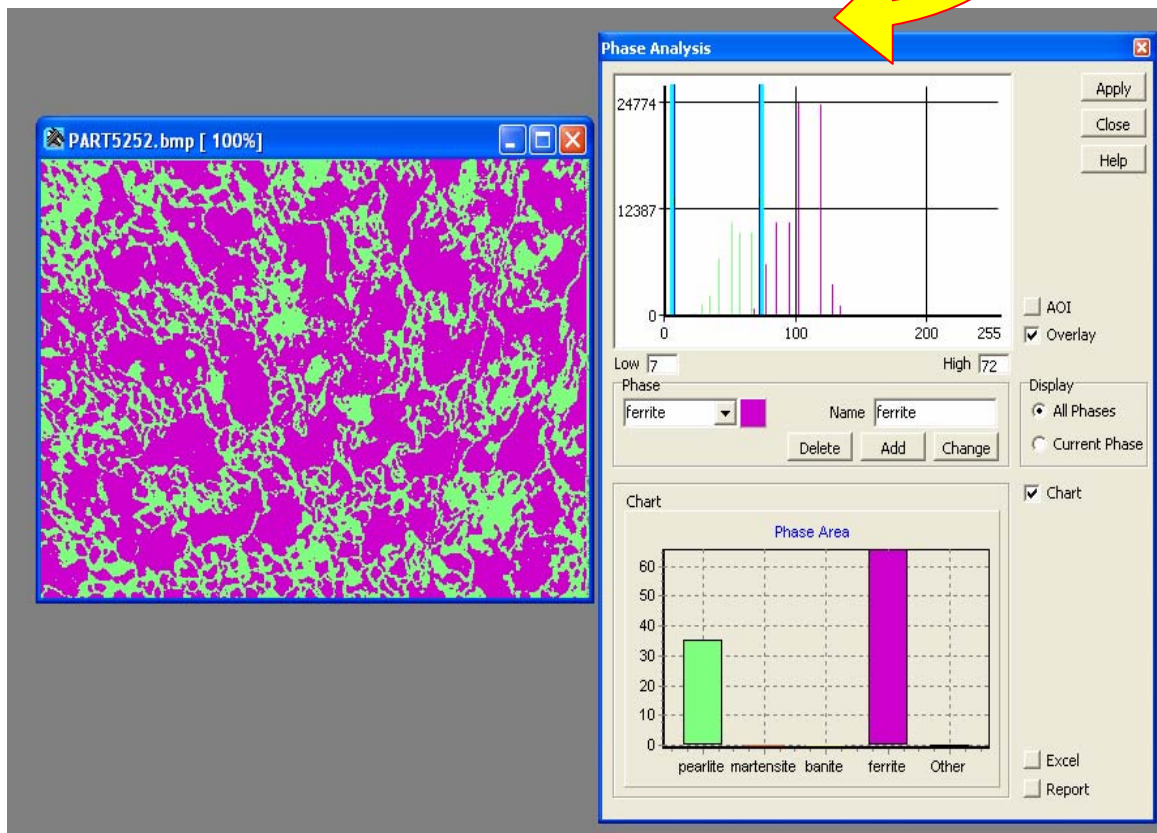


Fig.21 Result of Phase Analysis—

(Pearlite – 35% and Ferrite – 65%)

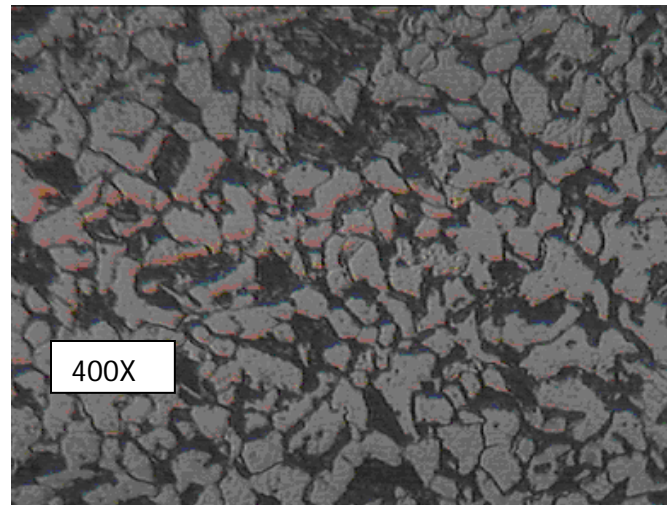


Fig. 22 Microstructure of Transition zone of sl no.3
(Current=600 amp, Voltage=38 volt, Travel Speed= 14.3mm/s)

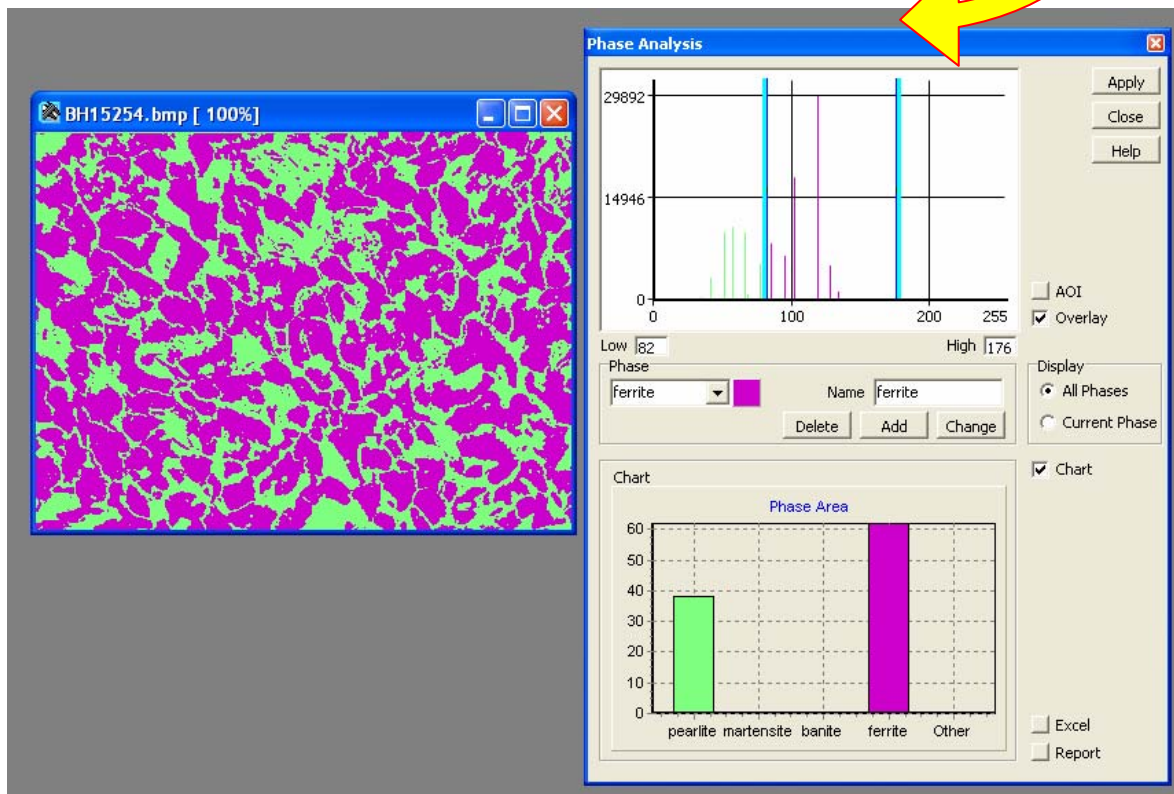


Fig.23 Result of Phase Analysis—
(Pearlite – 38% and Ferrite – 62%)

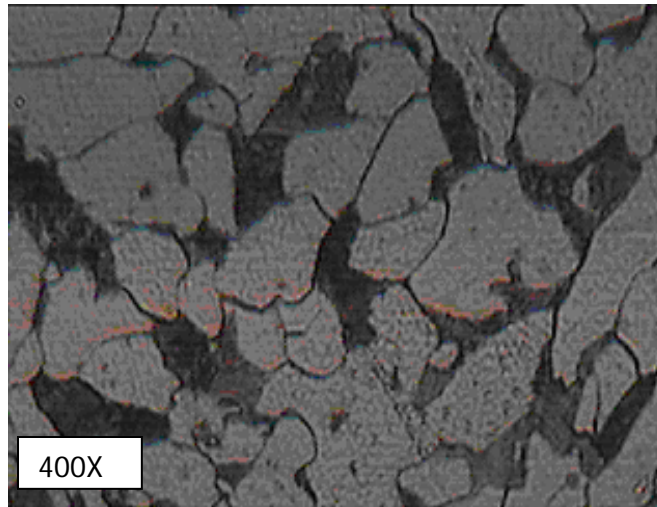


Fig. 24 Microstructure of Base metal (Mild steel)

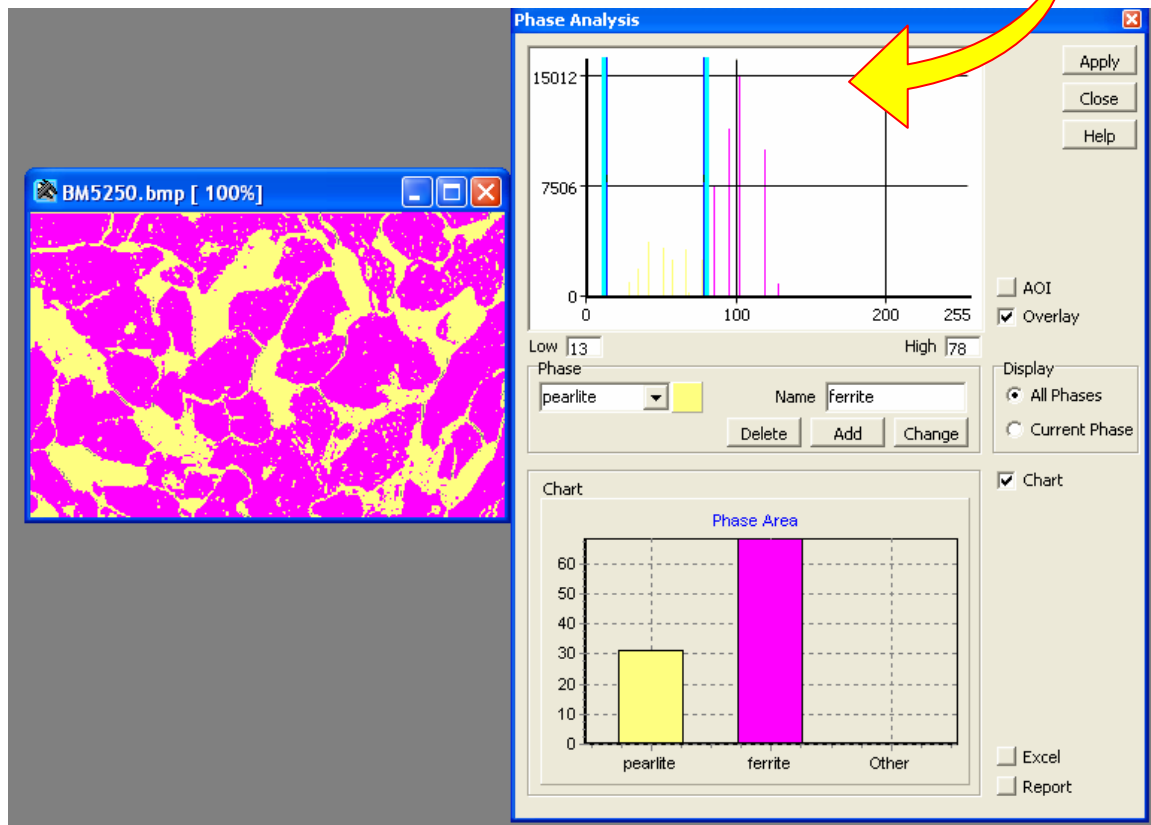
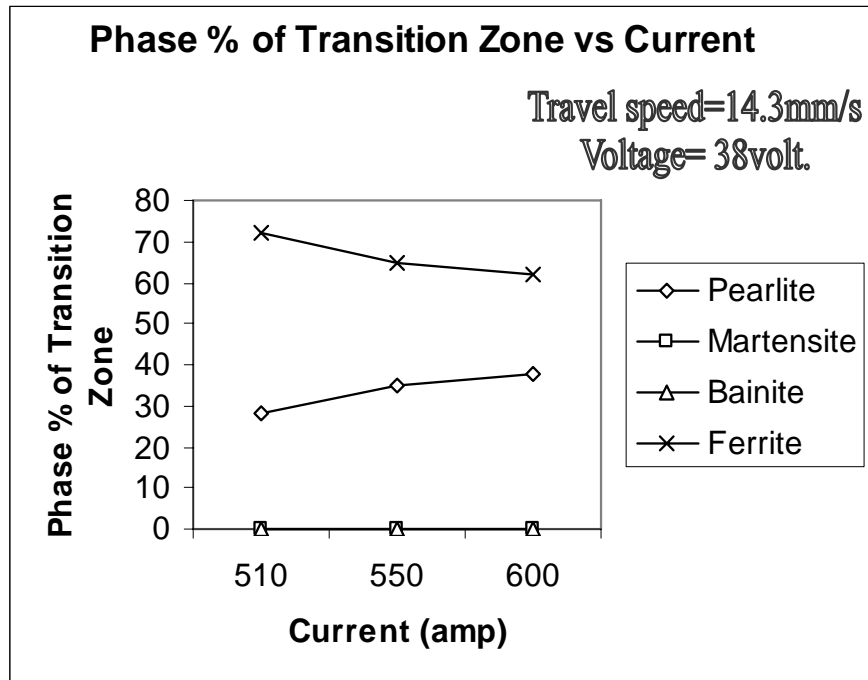


Fig.25 Result of Phase Analysis—

(Pearlite – 30% and Ferrite – 70%)

The following is the resulting Graph-



Graph 2. Drawn between percentage of Phases versus current for HAZ

➤ **Observations:**

The above graph shows the changes in the microstructure of Transition zone as the current was increased. Here we were observed that Pearlitic composition of the transition zone was increased but the percentage of ferrite, decreased.

3.1.2. Effect of increasing the arc voltage on phases

Travel speed (constant) = 14.3 mm/s

Current (constant) = 300 amp.

Voltage (increasing) = 35, 38, 41 & 44 volts

Sl. No.	Voltage (volts)	Current (amps)	Wire Feed (mm/s)	Travel Speed (mm/s)	HIR (j/mm)	Weld Brnll. Hardness	HAZ1 Brnll. Hrd.	HAZ2 Brnll. Hrd.	HAZ3 Brnll. Hrd.	Base-Metal Hrd.
4	35	300	65.8	14.3	734.3	241	216	195	186	160
5	38	300	65.8	14.3	797.2	255	229	201	190	158
6	41	300	65.8	14.3	839	261	232	216	201	159
7	44	300	65.8	14.3	944	269	236	221	209	160

Table 2. Here voltage and travel speed were taken as constant and wire feed i.e. Voltage was increased.

Phase analysis images of Fusion zone:

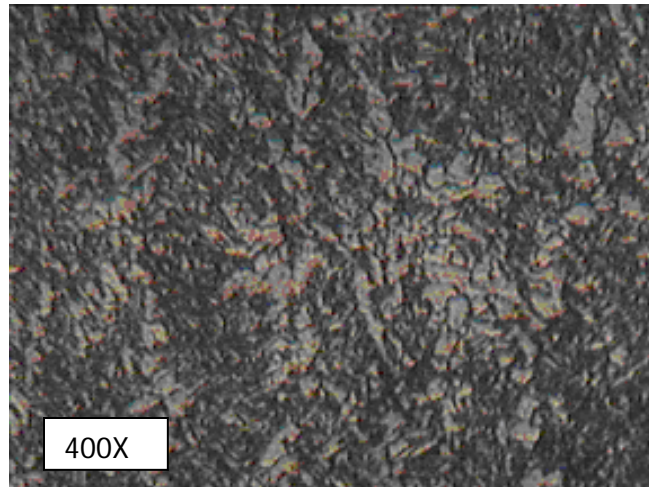


Fig. 26 Microstructure of fusion zone, SL no.4

(Voltage = 35volt, Current= 300amp, Travel Speed= 14.3mm/s)

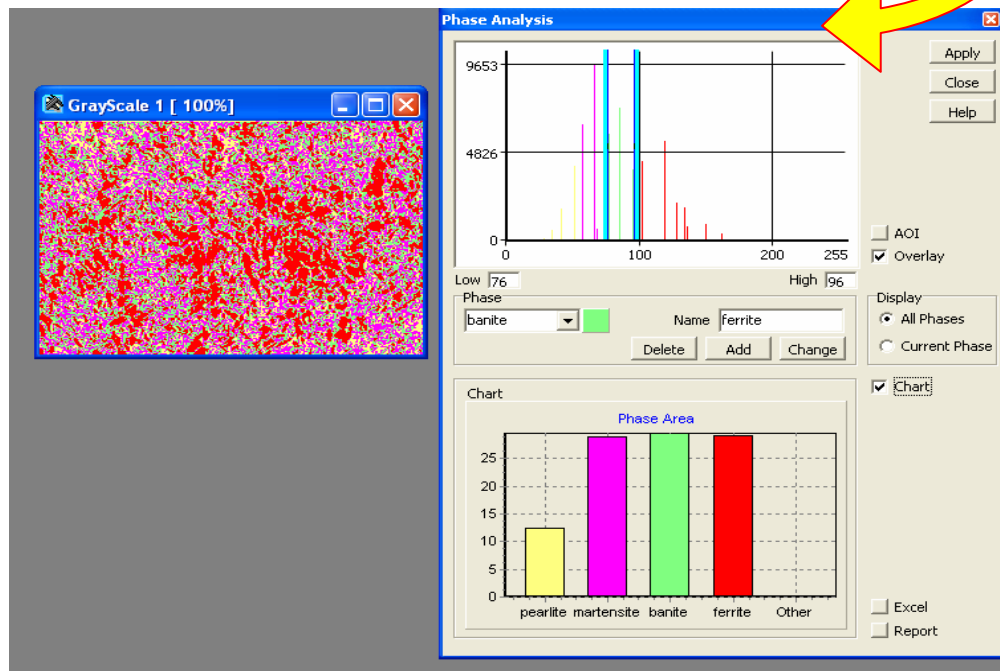


Fig.27 Result of Phase Analysis—

(Pearlite – 12%, Martensite- 28% , Bainite – 30%, and Ferrite – 30%)

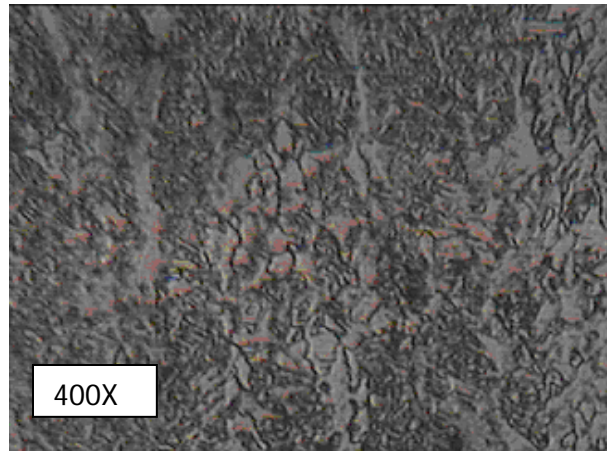


Fig. 28 Microstructure of fusion zone, Sl no. 5

(Voltage = 38volt, Current= 300amp, Travel Speed= 14.3mm/s)

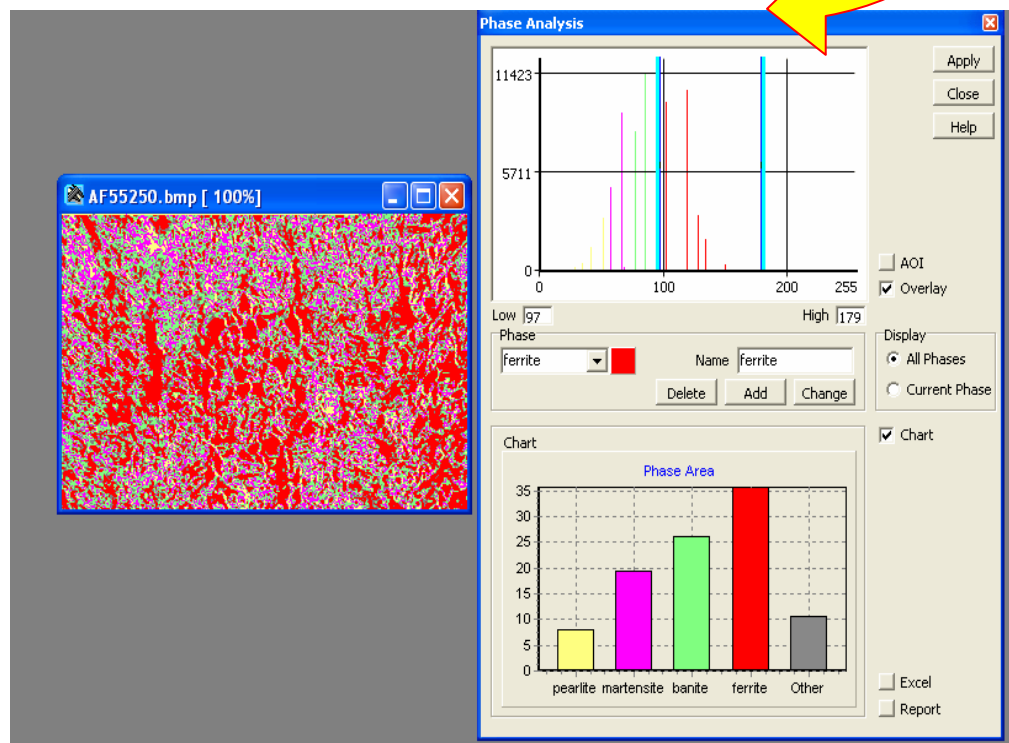


Fig.29 Result of Phase Analysis—

(Pearlite – 09%, Martensite- 22%, Bainite – 28%, and Ferrite – 38%)

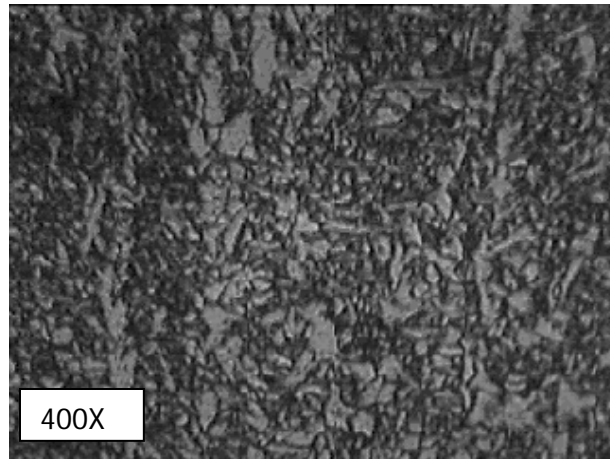


Fig. 30 Microstructure of fusion zone, Sl no. 6

(Voltage = 41volt, Current= 300amp, Travel Speed= 14.3mm/s)

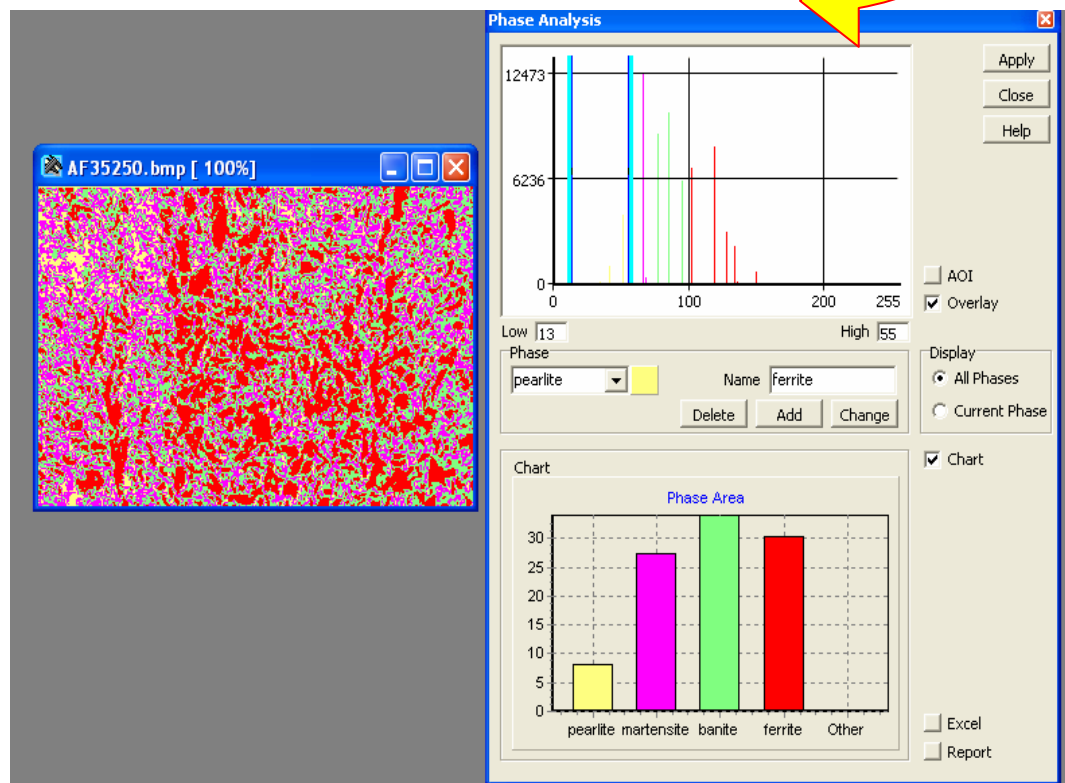


Fig.31 Result of Phase Analysis—

(Pearlite – 08%, Martensite- 27% , Bainite – 35%, and Ferrite – 30%)

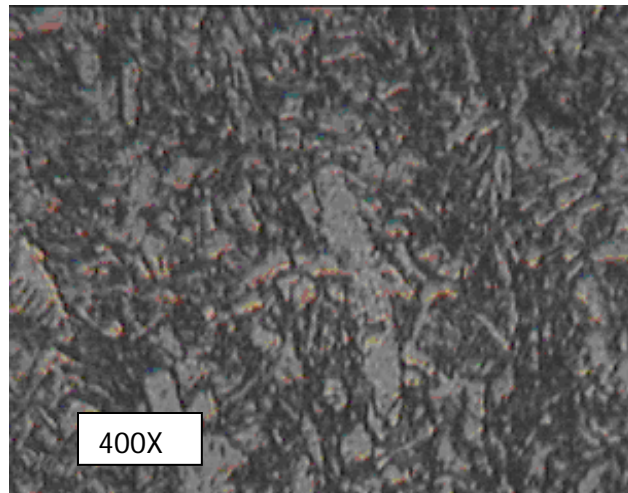


Fig. 32 Microstructure of fusion zone, Sl no. 7

(Voltage = 44volt, Current= 300amp, Travel Speed= 14.3mm/s)

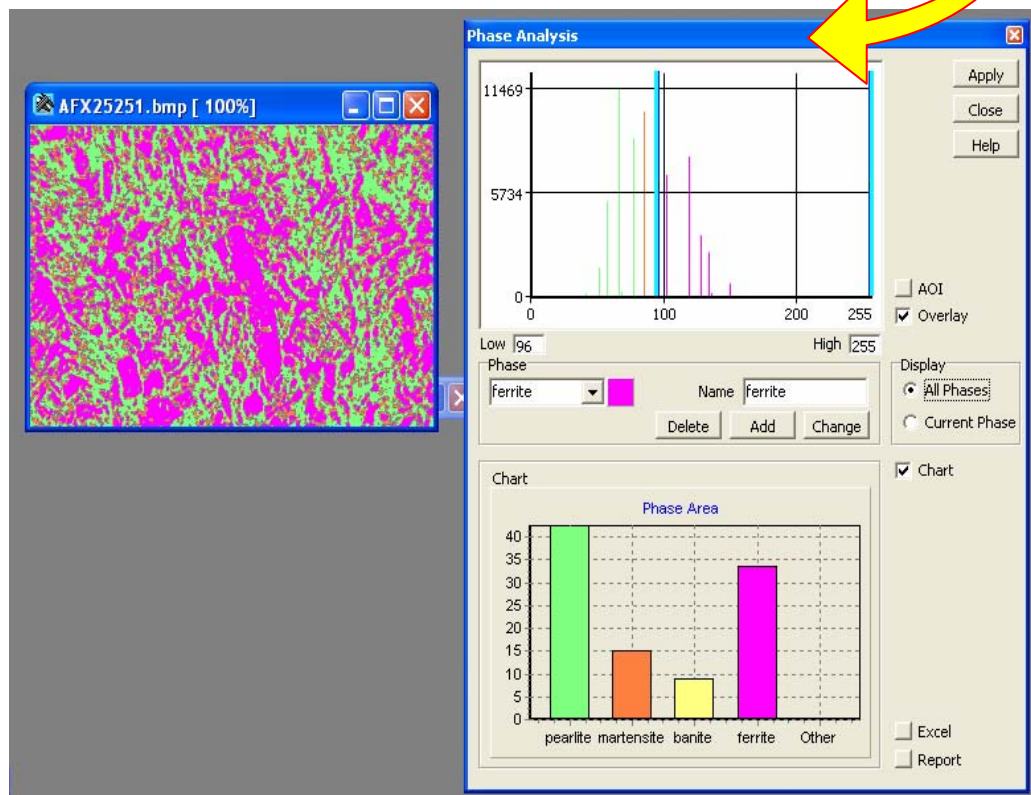
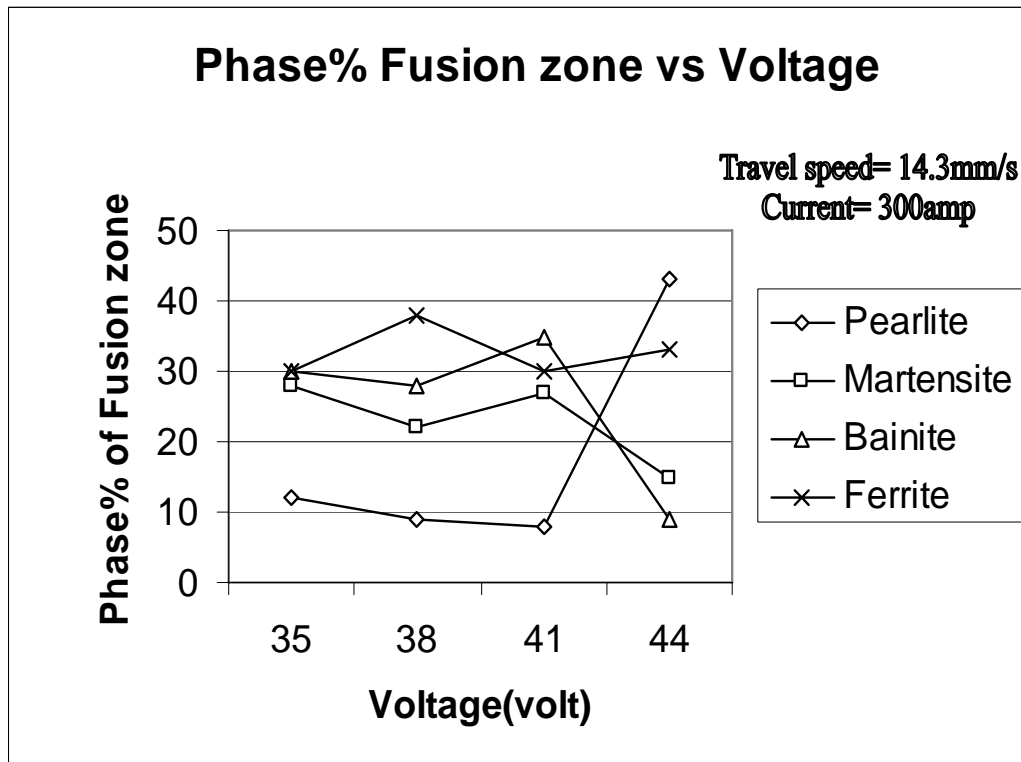


Fig.33 Result of Phase Analysis—

(Pearlite – 43%, Martensite- 15%, Bainite –9%, and Ferrite – 33%)

The following is the resulting Graph-



Graph 4. Drawn between percentage of Phases versus Voltage for Fusion zone

➤ **Observations:**

The above graph shows the changes in microstructure of the fusion zone as the Voltage was increased. Here we were observed various changes as the Pearlite was firstly decreased and then increased drastically, martensite & bainite decreased but the ferrite was approximately at the same percentage.

Phase analysis picture of HAZ:

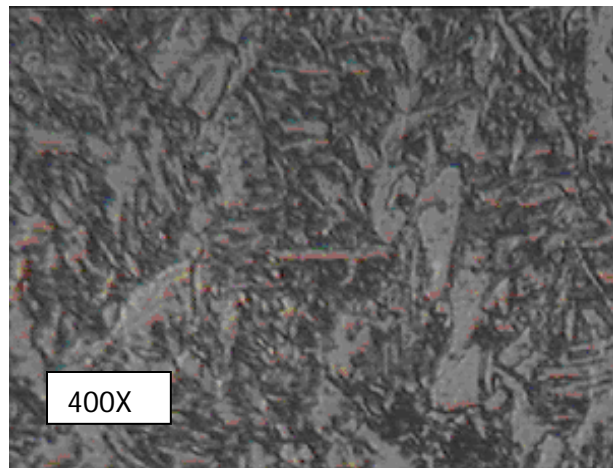


Fig. 34 Microstructure of HAZ, SL no. 4

(Voltage = 35volt, Current= 300amp, Travel Speed= 14.3mm/s)

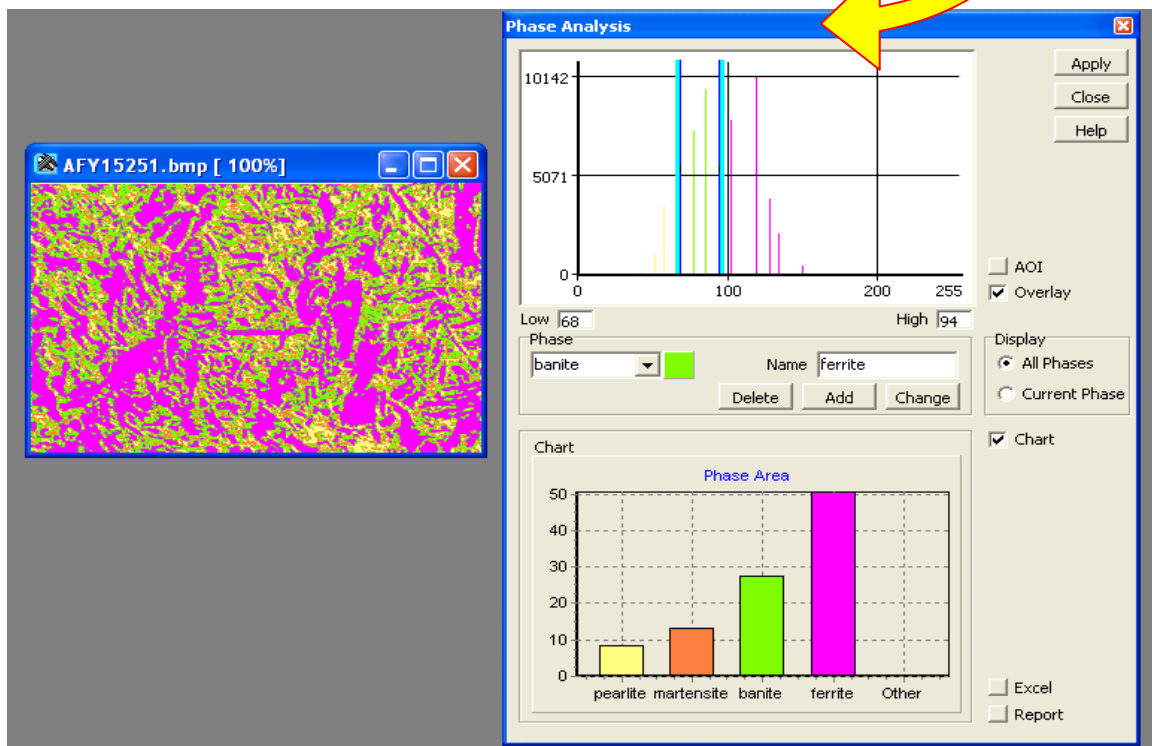


Fig.35 Result of Phase Analysis—

(Pearlite – 9%, Martensite- 12% , Bainite – 28%, and Ferrite – 51%)

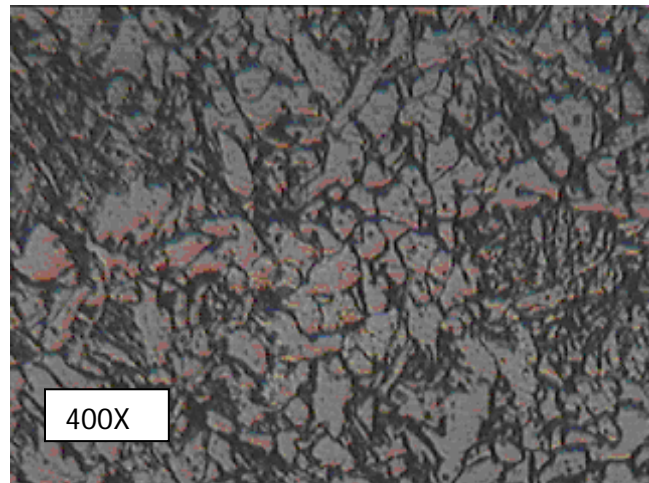


Fig. 36 Microstructure of HAZ, Sl no. 5

(Voltage = 38volt, Current= 300amp, Travel Speed= 14.3mm/s)

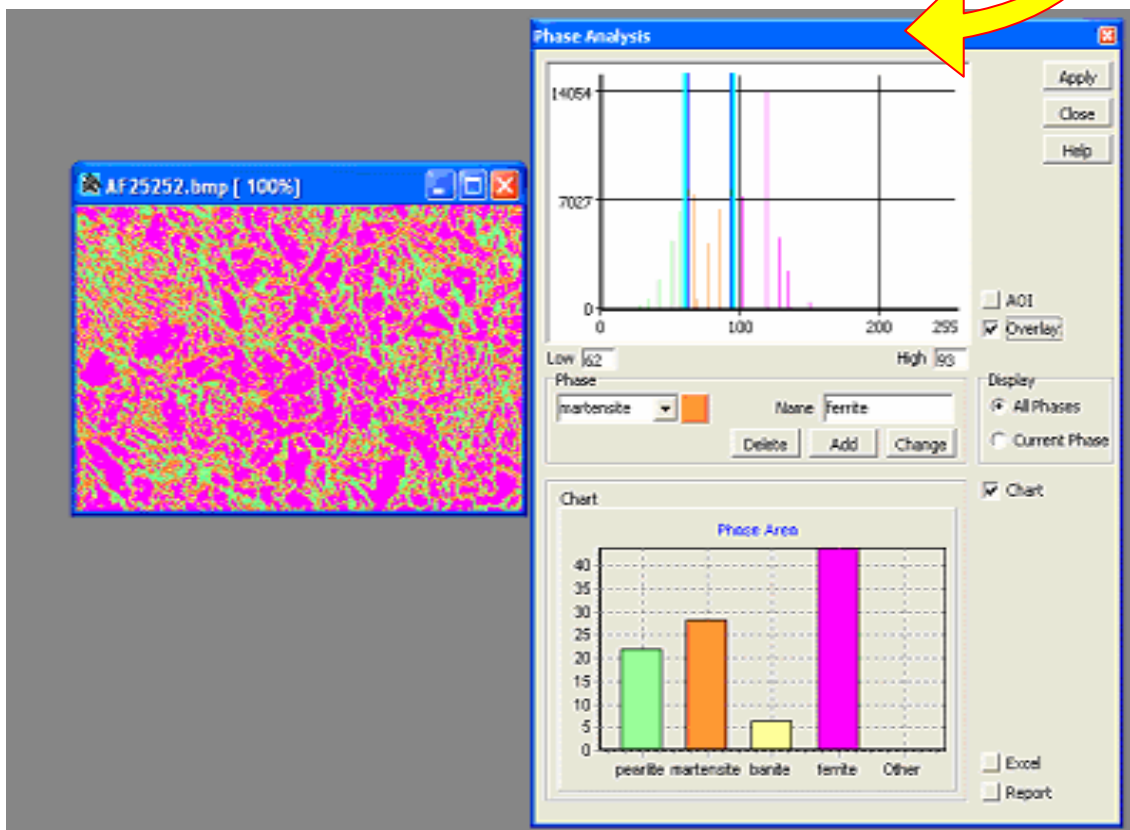


Fig.37 Result of Phase Analysis—

(Pearlite – 22%, Martensite- 28% , Bainite – 7%, and Ferrite – 43%)

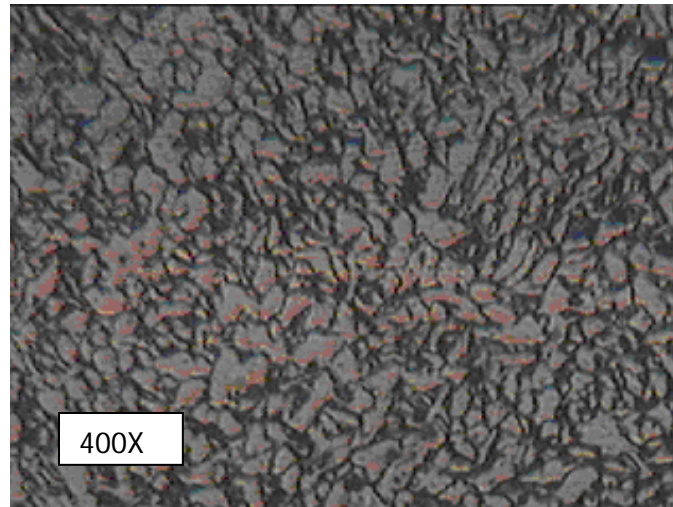


Fig. 38 Microstructure of HAZ, Sl no. 6

(Voltage = 41volt, Current= 300amp, Travel Speed= 14.3mm/s)

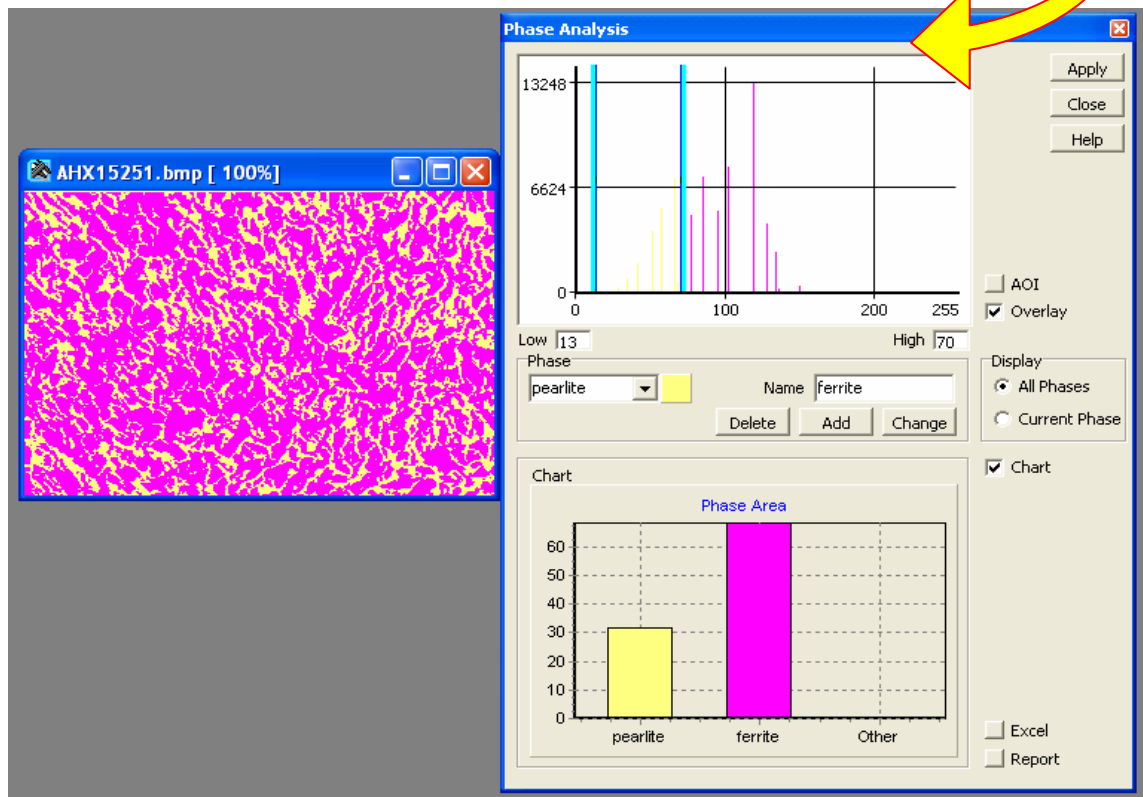


Fig.39 Result of Phase Analysis—

(Pearlite – 32%, Ferrite – 68%)

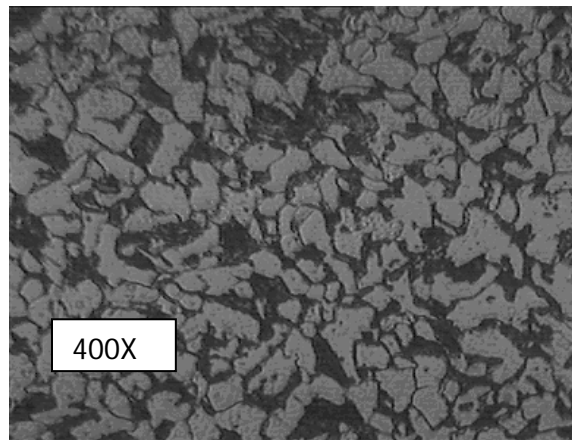


Fig. 40 Microstructure of HAZ, Sl no. 7

(Voltage = 44 volt, Current= 300amp, Travel Speed= 14.3mm/s)

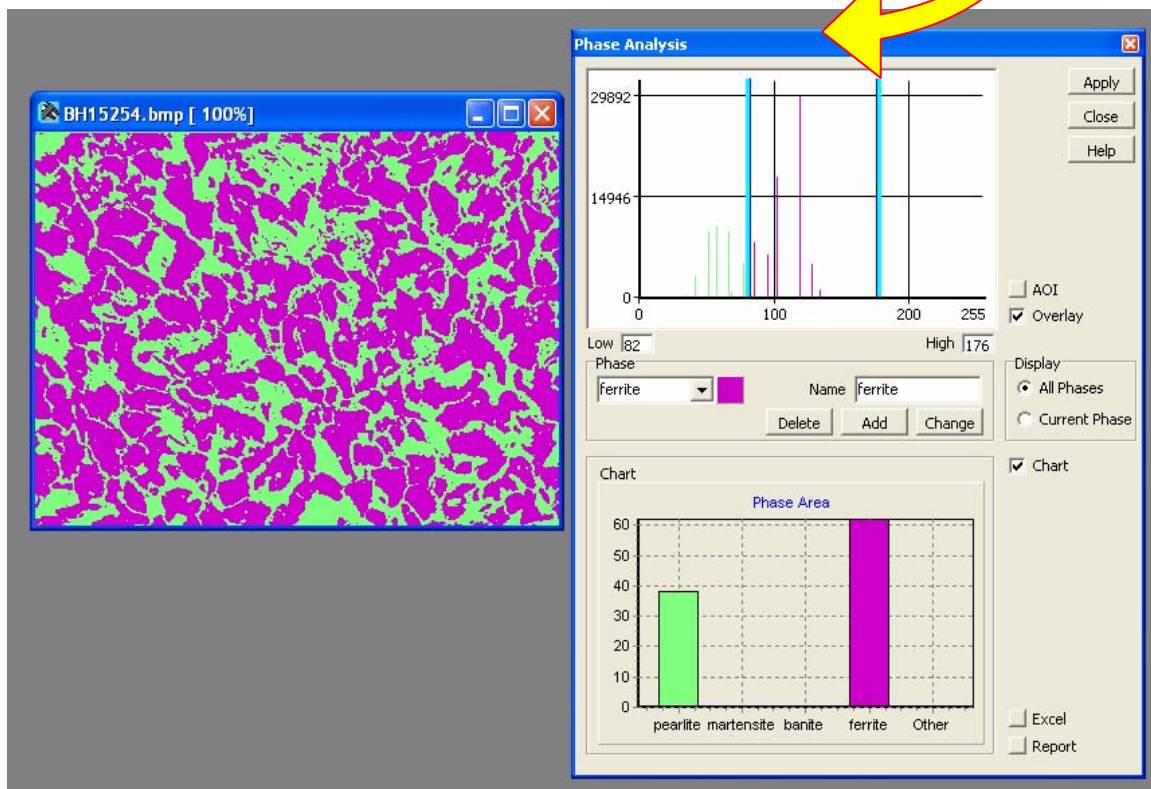
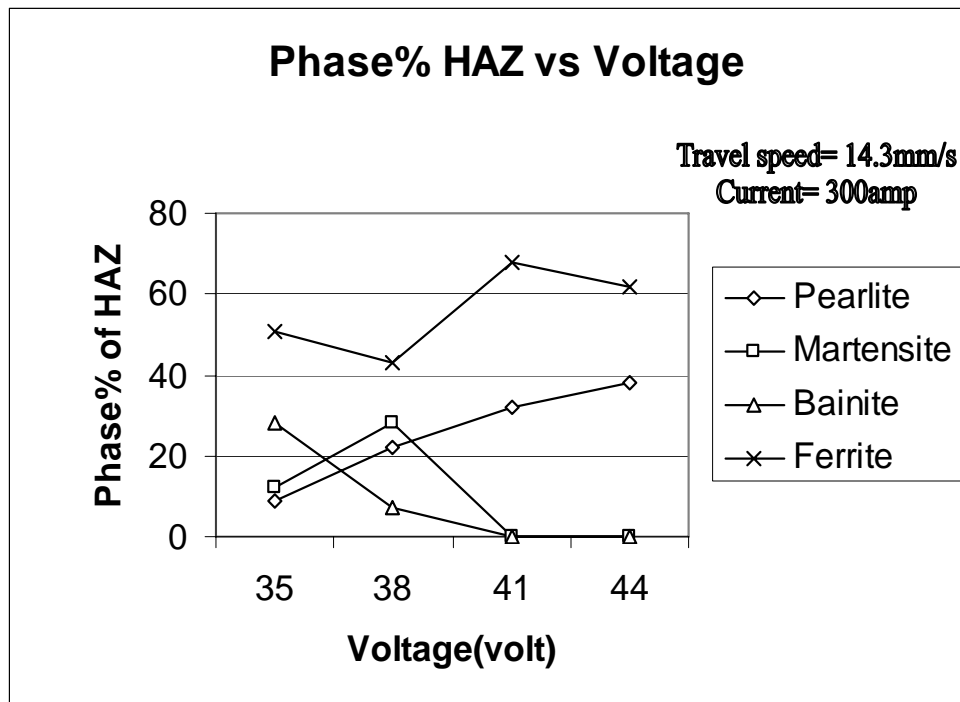


Fig.41 Result of Phase Analysis—

(Pearlite – 38%, Ferrite – 62%)

The following is the resulting Graph-



Graph 5. Drawn between percentage of Phases versus Voltage for HAZ

➤ **Observations:**

The above graph shows the changes in microstructure of the HAZ as the Voltage was increased. Here we were observed various changes as Pearlite was increasing and martensite & bainite were decreasing but the ferrite was increasing.

Phase analysis images of Transition zone:

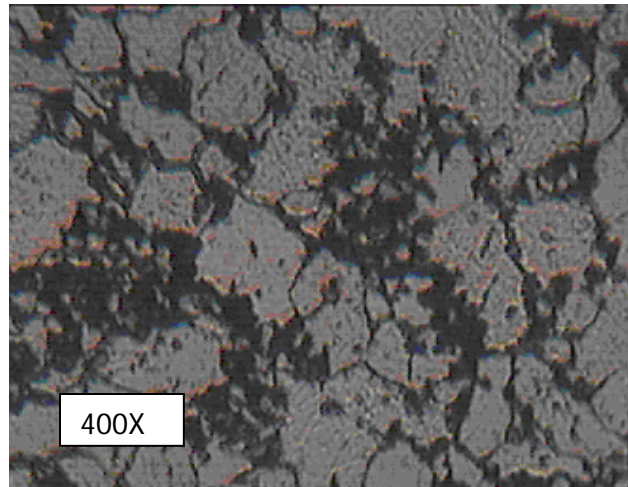


Fig. 42 Microstructure of Transition zone Sl no. 4

(Voltage = 35volt, Current= 300amp, Travel Speed= 14.3mm/s)

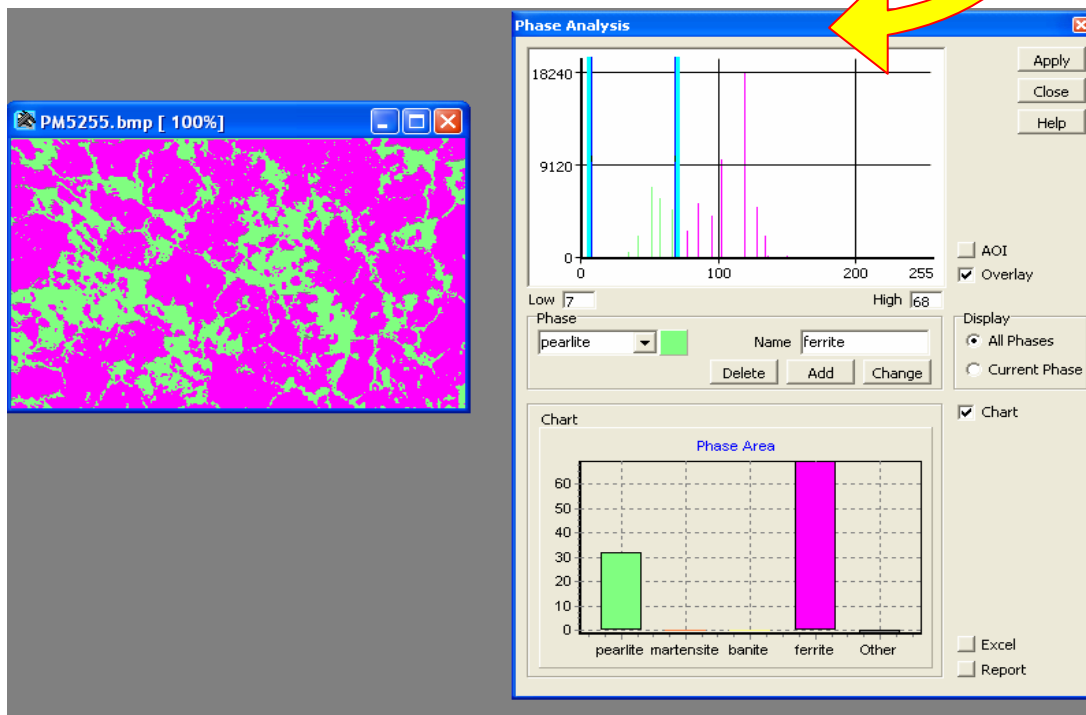


Fig.43 Result of Phase Analysis—

(Pearlite – 31%, Ferrite – 69%)

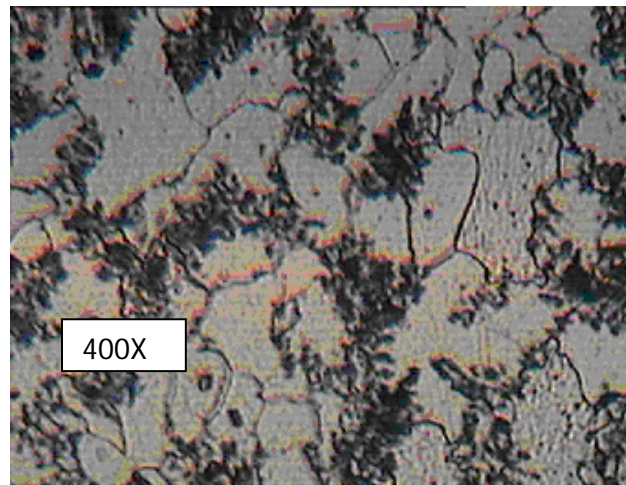


Fig. 44 Microstructure of Transition zone, Sl no. 5

(Voltage = 38volt, Current= 300amp, Travel Speed= 14.3mm/s)

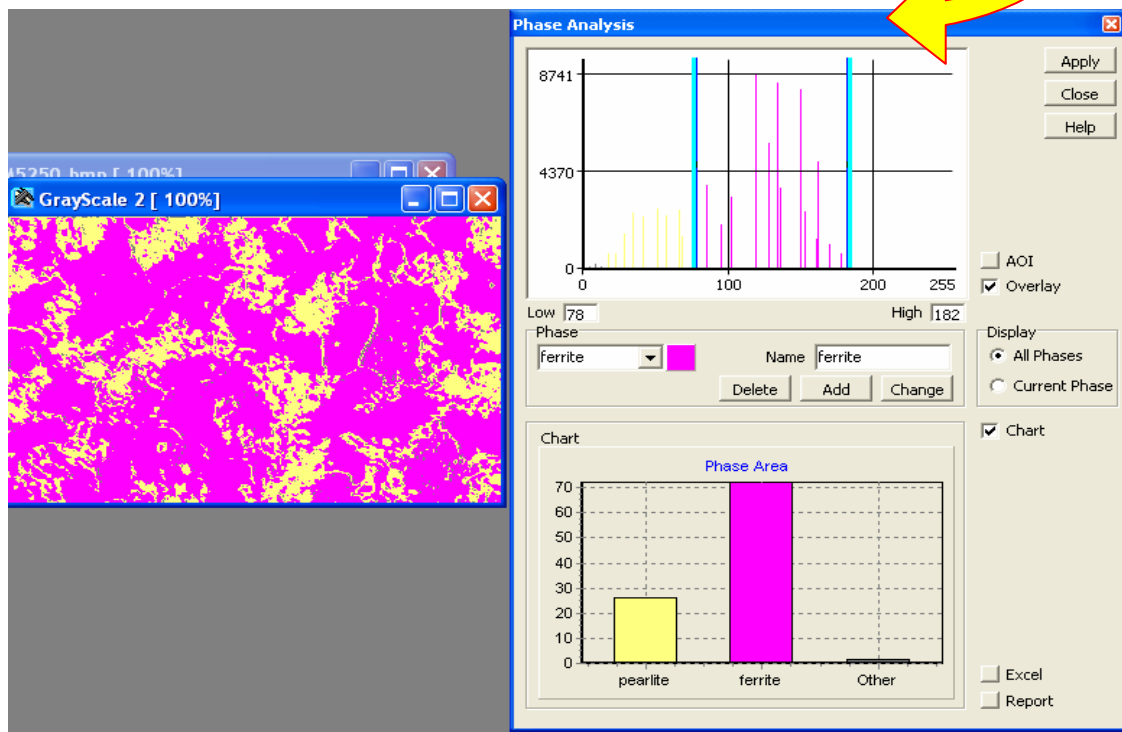


Fig.45 Result of Phase Analysis—

(Pearlite – 28%, Ferrite – 72%)

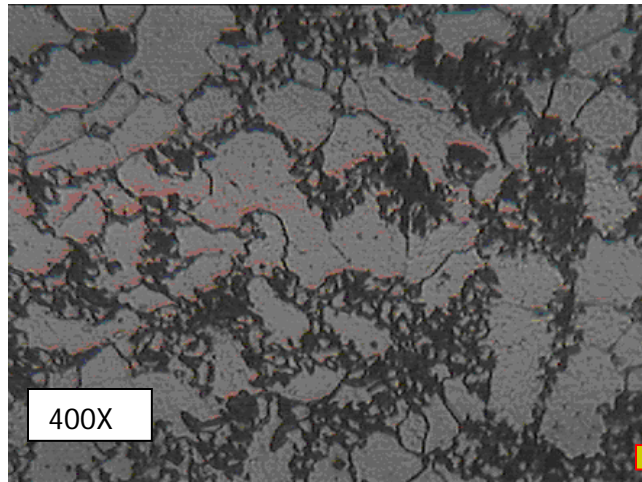


Fig. 46 Microstructure of Transition zone, Sl no. 6

(Voltage = 41volt, Current= 300amp, Travel Speed= 14.3mm/s)

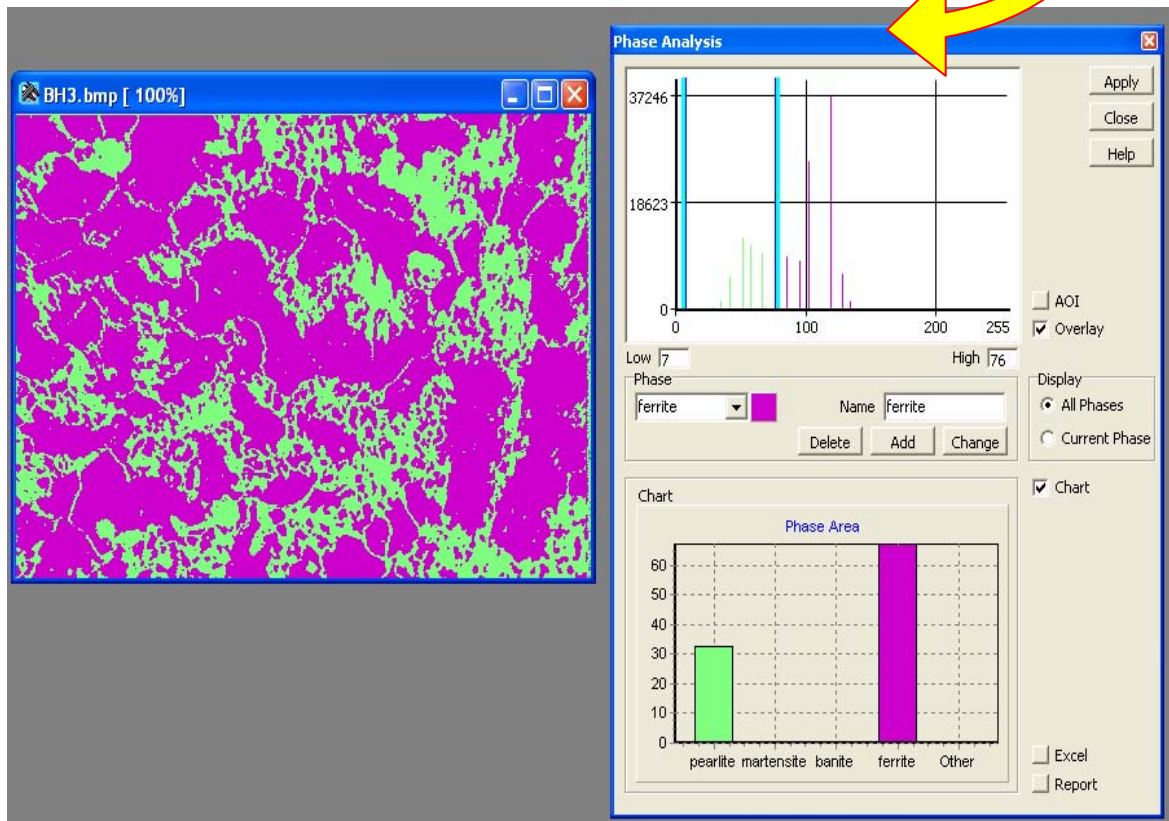


Fig.47 Result of Phase Analysis—

(Pearlite – 32%, Ferrite – 68%)

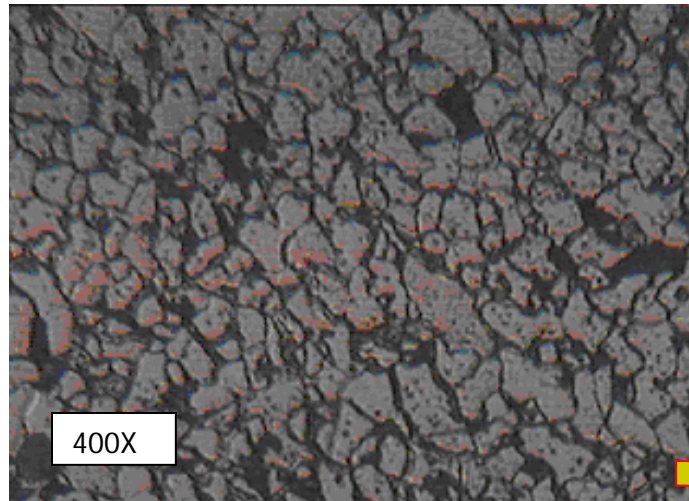


Fig.48 Microstructure of Transition zone, Sl no. 7

(Voltage = 44volt, Current= 300amp, Travel Speed= 14.3mm/s)

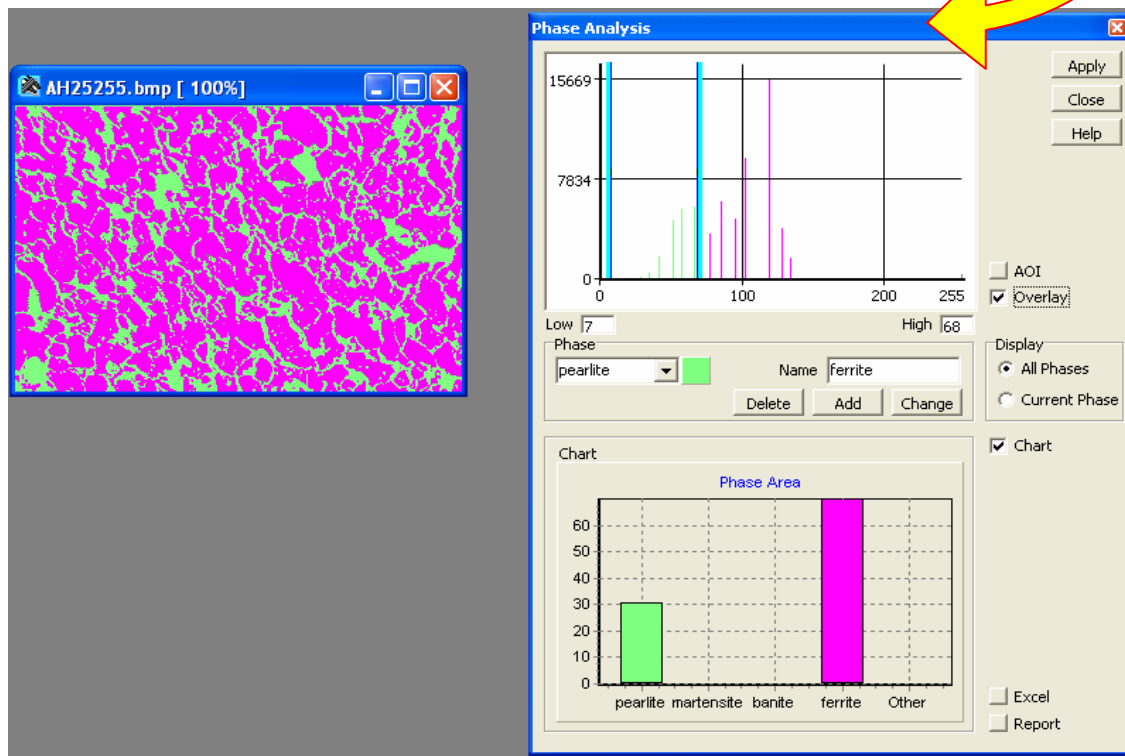
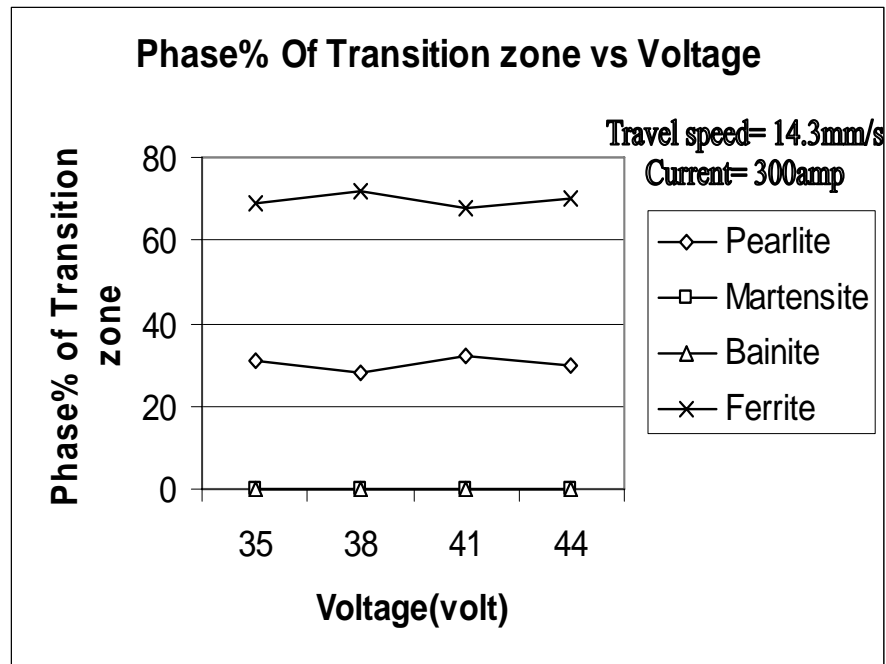


Fig.49 Result of Phase Analysis—

(Pearlite – 30%, Ferrite – 70%)

The following is the resulting Graph-



Graph 6. Drawn between percentages of Phases versus Voltage for Transition Zone

➤ **Observations:**

The above graph shows the changes in microstructure of the Transition zone as the voltage was increased. Here we were observed small changes as Pearlite was decreasing and increasing slightly, ferrite was following the apposite pattern of pearlite. There were no % of martensite and bainite in this zone.

3.2.1 Effect of welding current on grain size:

The following are the analysis results of grain size when the current was Increased-

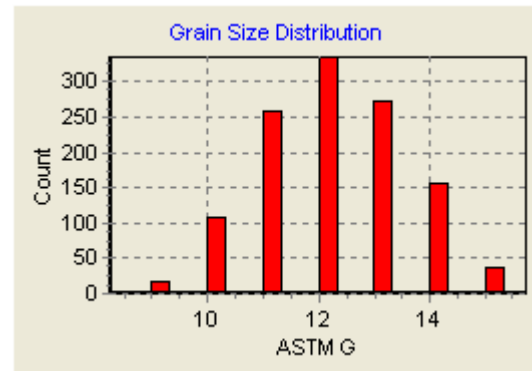
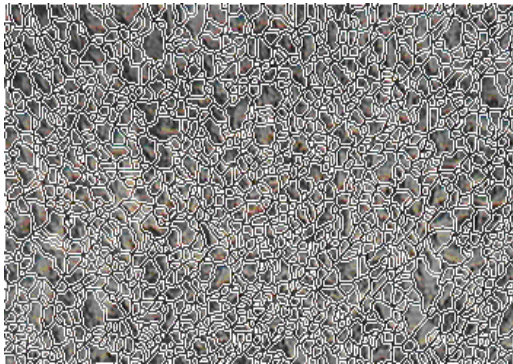


Fig.50 Analyzed picture of fusion zone, sl no.1 **Chart 1.**Distribution of ASTM grain over area

Result of grain analysis, ASTM Grain = 11.53

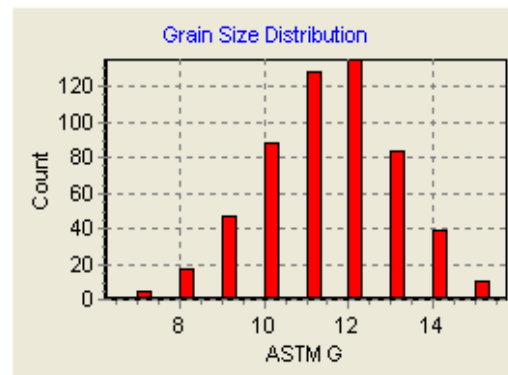
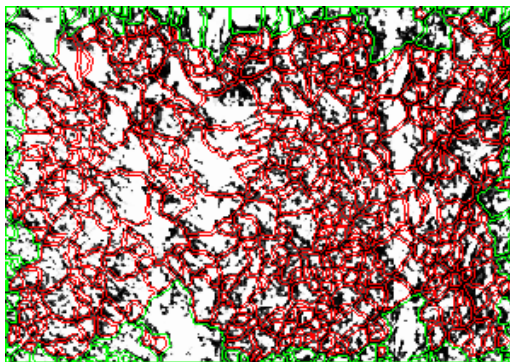


Fig.51 Analyzed picture of fusion zone, sl no.2 **Chart 2.**Distribution of grain over area

Result of grain analysis, ASTM Grain = 10.53

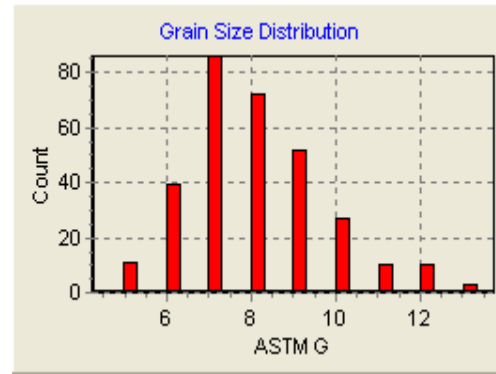
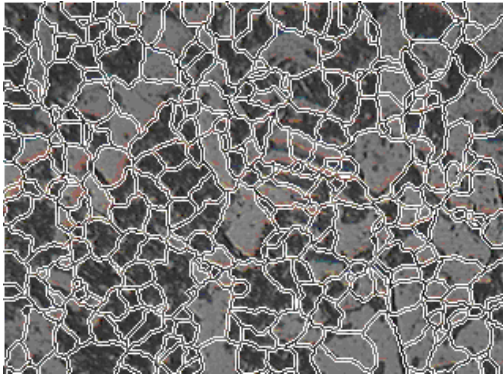


Fig.52 Analyzed picture of fusion zone sl no.3 **Chart 3.**Distribution of grain over area
Result of grain analysis, ASTM Grain = 7.42

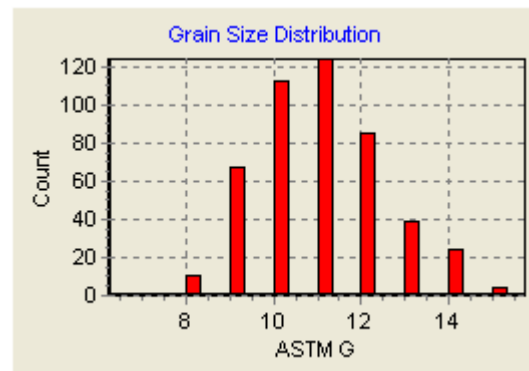
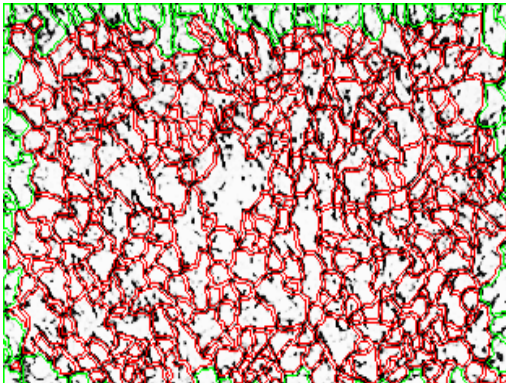


Fig.53 Analyzed picture of HAZ sl no.1 **Chart 4.**Distribution of grain over area
Result of grain analysis, ASTM Grain = 10.35

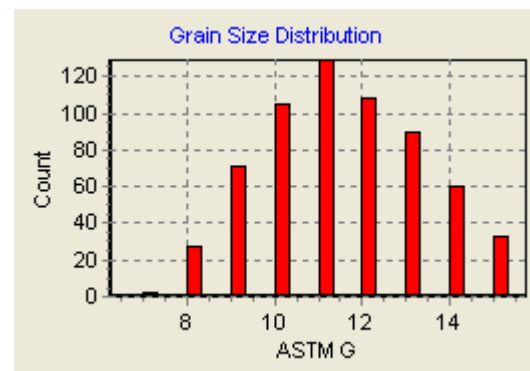
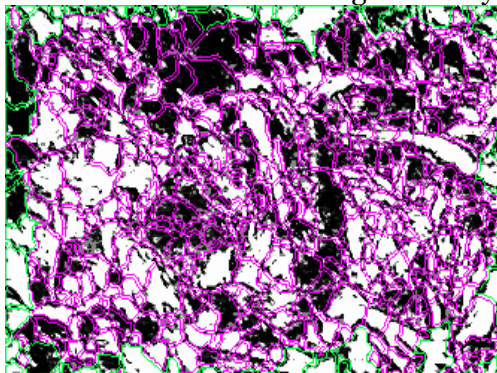


Fig.54 Analyzed picture of HAZ sl no.2 **Chart 5.**Distribution of grain over area
Result of grain analysis, ASTM Grain = 10.48

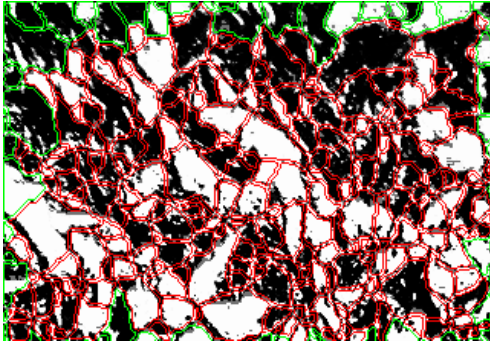


Fig.55 Analyzed picture of HAZ sl no.3

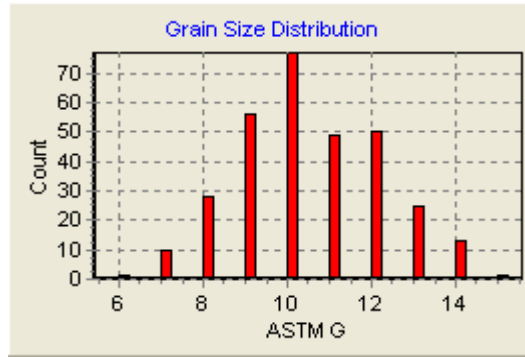


Chart 6..Distribution of grain over area

Result of grain analysis, ASTM Grain = 9.63

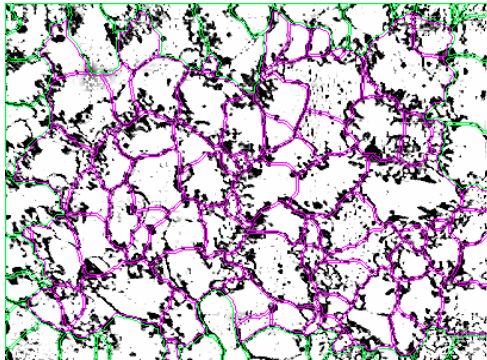


Fig.56 Analyzed pict. of Transition zone sl no.1

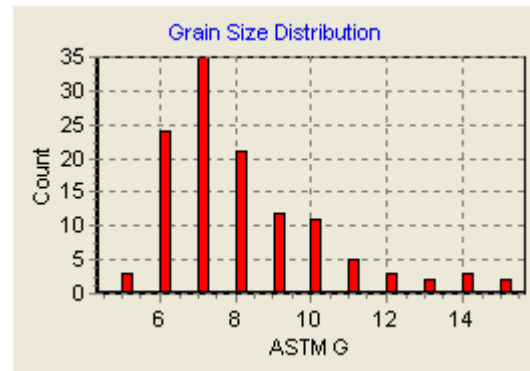


Chart 7.Distribution of grain over area

Result of grain analysis, ASTM Grain = 7.29

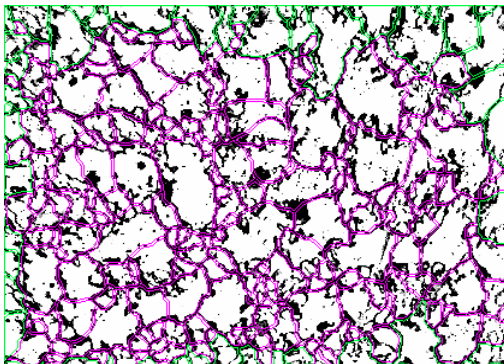


Fig.57 Analyzed pic. of Transition zone sl. no.2

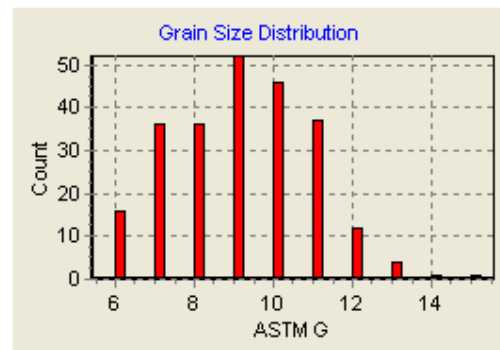


Chart 8. Distribution of grain over area

Result of grain analysis, ASTM Grain = 8.36

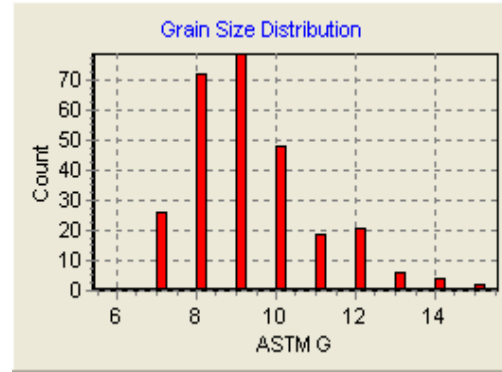
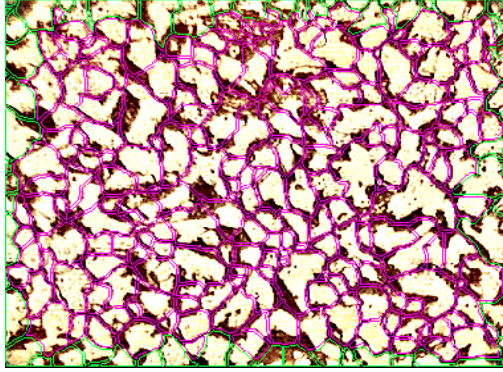


Fig.58 Analyzed pic. of Transition zone sl no.3

Chart 9.Distribution of grain over area

Result of grain analysis, ASTM Grain = 8.74

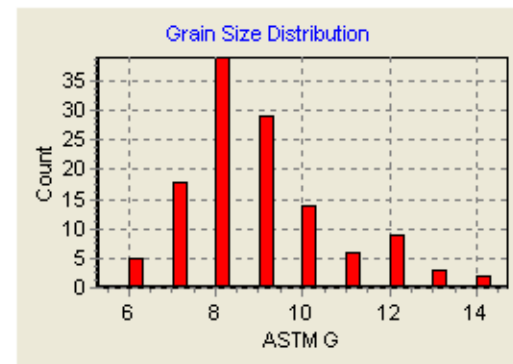
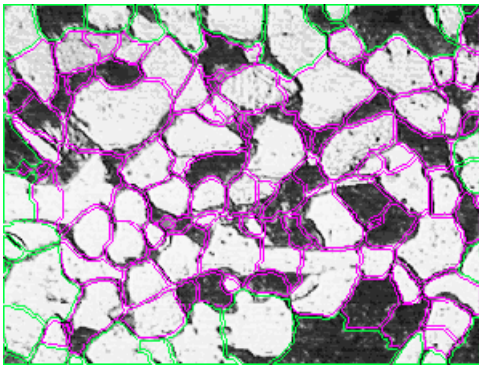


Fig.59 Analyzed picture of base metal

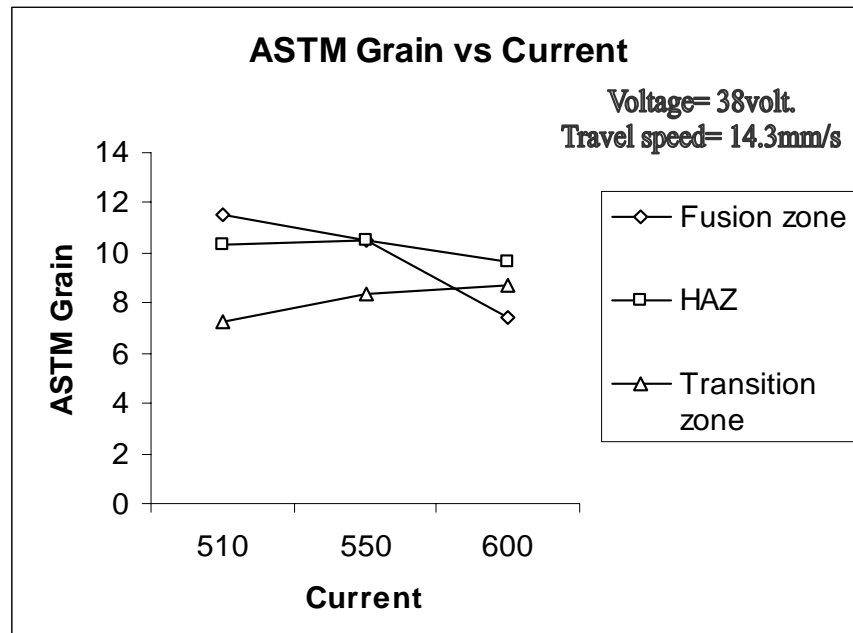
Chart 10.Distribution of grain over area

Result of grain analysis, ASTM Grain = 7

Here we were found that the grain size of the base metal is larger than of weld metal and HAZ.

The following graph shows the result of increasing current on grain size of

Various zone:--



Graph 7. Drawn between ASTM Grain versus Current Keeping other parameter constant.

Here we were observed small changes in grain size of HAZ area but in fusion zone the grain size was increased considerably and for transition zone the grain size reduced slightly because of change of pearlite grain into ferrite.

3.2.2 Effect of welding voltage on grain size

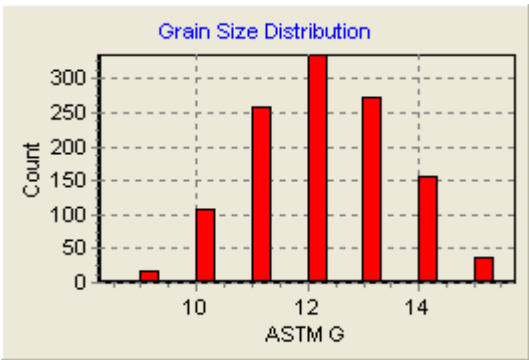
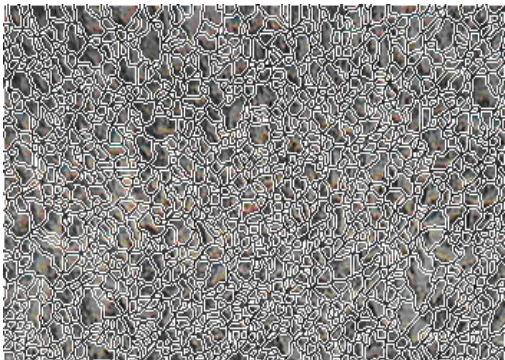


Fig.60 Analyzed picture of fusion zone sl no.4 **Chart 11.** Distribution of grain over area
Result of grain analysis, ASTM Grain = 11.51

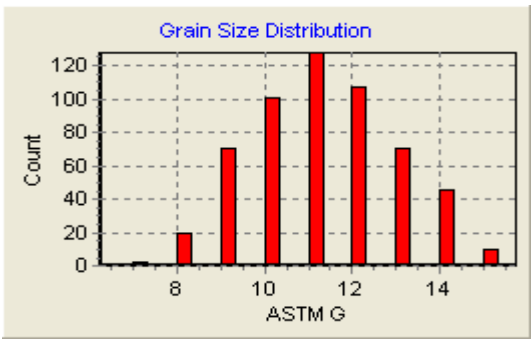
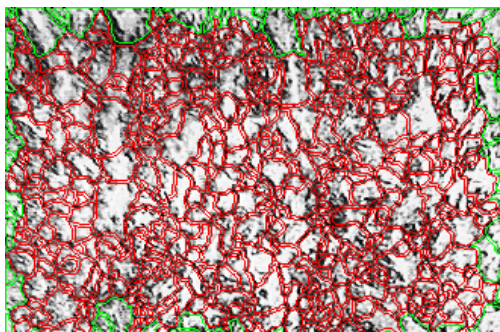


Fig.61 Analyzed picture of fusion zone sl no. 5 **Chart 12.** Distribution of grain over area
Result of grain analysis, ASTM Grain = 10.42

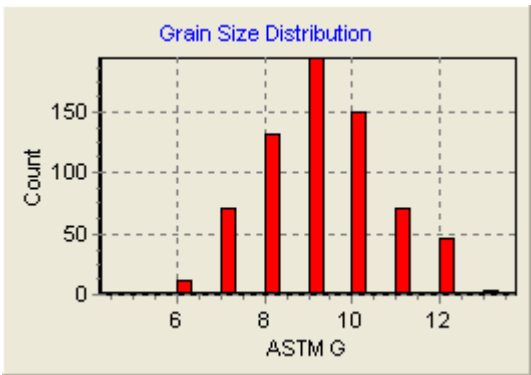
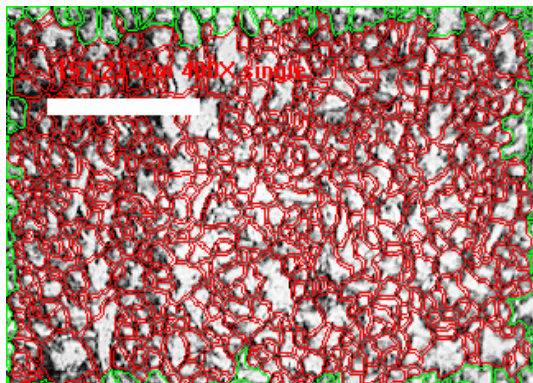


Fig.62 Analyzed pic. of fusion zone sl no. 6 **Chart 13.** Distribution of grain over area
Result of grain analysis, ASTM Grain = 9.56

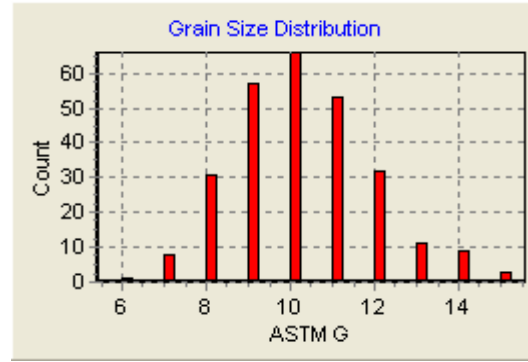
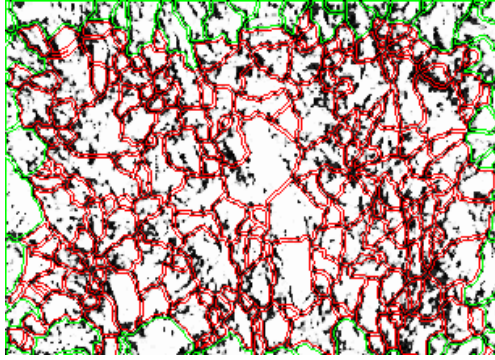


Fig.63 Analyzed pic. of fusion zone sl no. 7 **Chart 14.** Distribution of grain over area
Result of grain analysis, ASTM Grain = 8.89

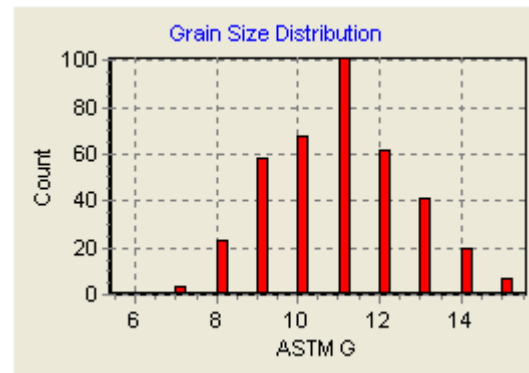
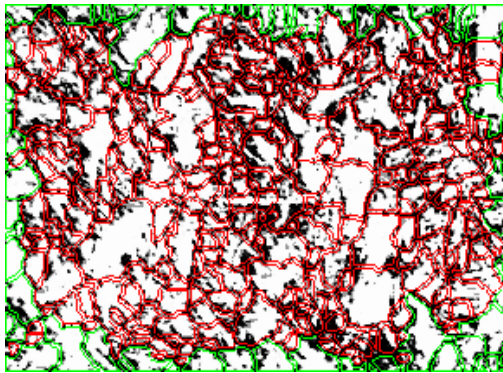


Fig.64 Analyzed picture of HAZ sl no. 4 **Chart 15.** Distribution of grain over area
Result of grain analysis, ASTM Grain = 10.12

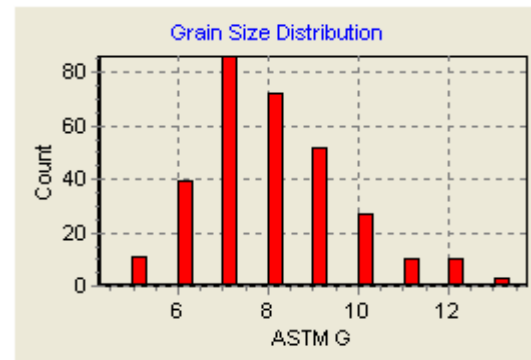
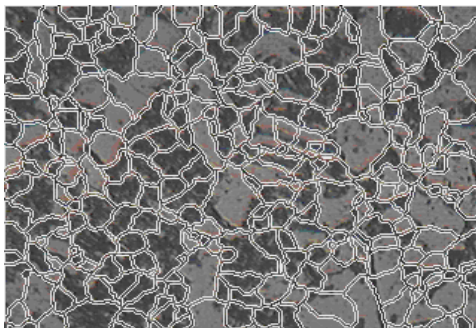


Fig.65 Analyzed picture of HAZ sl no. 5 **Chart 16.** Distribution of grain over area
Result of grain analysis, ASTM Grain = 8.52

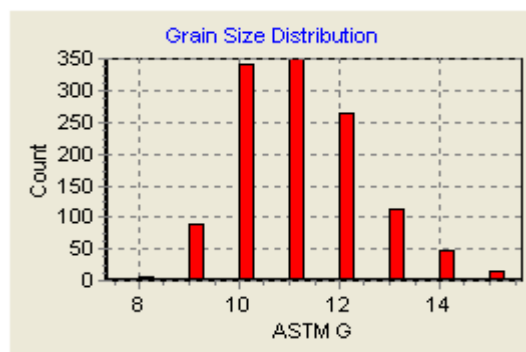
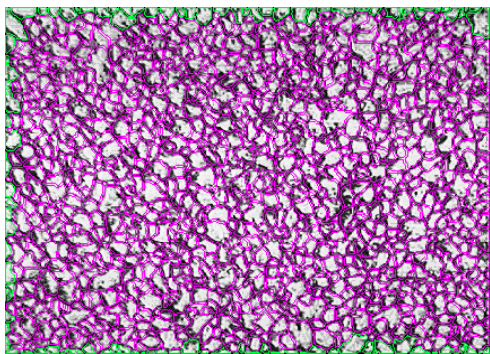


Fig.66 Analyzed picture of HAZ sl no. 6

Chart 17. Distribution of grain over area

Result of grain analysis, ASTM Grain = 10.73

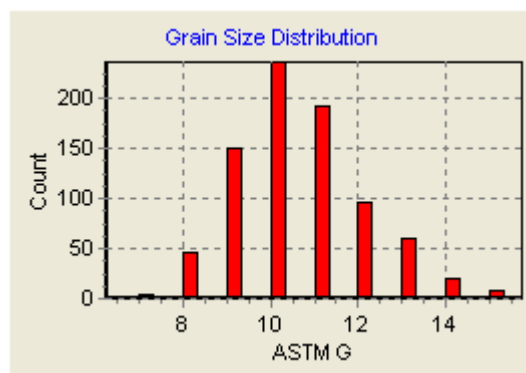
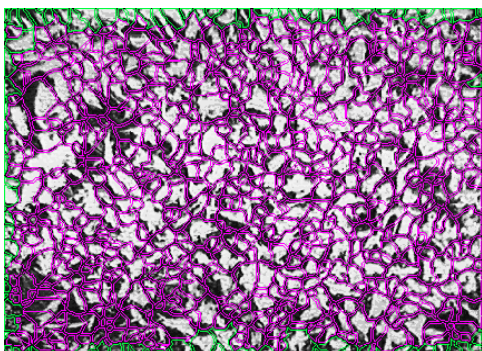


Fig.67 Analyzed pic. of HAZ sl no. 7

Chart 18. Distribution of grain over area

Result of grain analysis, ASTM Grain = 10.

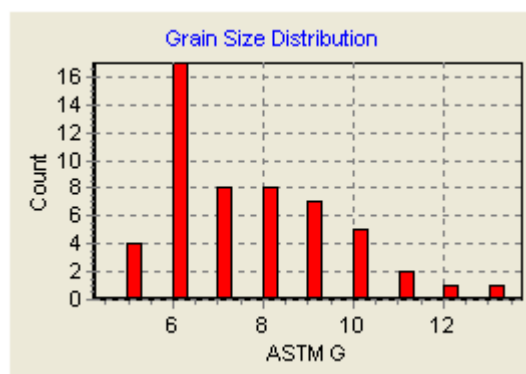
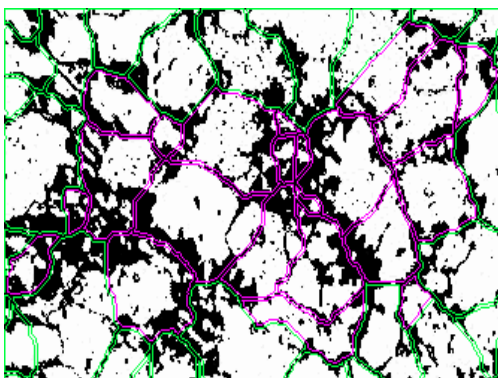


Fig.68 Analyzed pic. of Transition zone sl. no.4

Chart 19. Distribution of grain over area

Result of grain analysis, ASTM Grain = 6.87

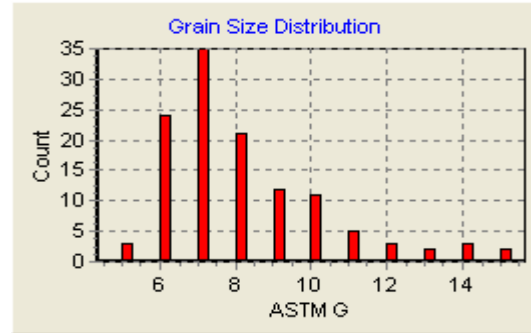
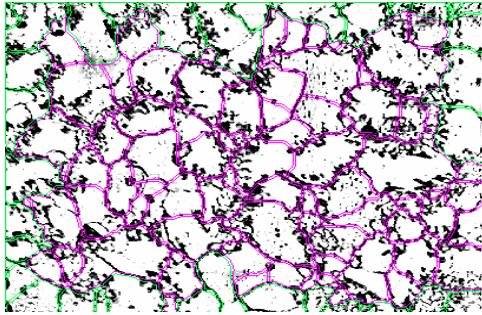


Fig.69 Analyzed pic. of Transition zone sl. no.5

Chart 20. Distribution of grain over area

Result of grain analysis, ASTM Grain = 7.29

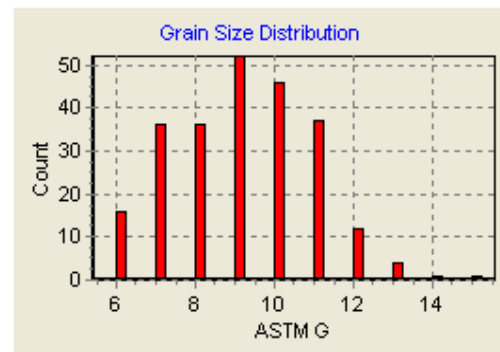
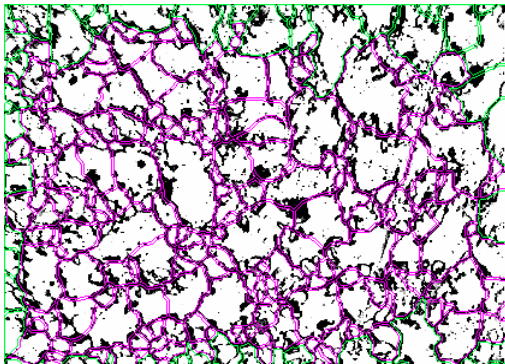


Fig.70 Analyzed pic. of Transition zone sl. no.6

Chart 21. Distribution of grain over area

Result of grain analysis, ASTM Grain = 8.36

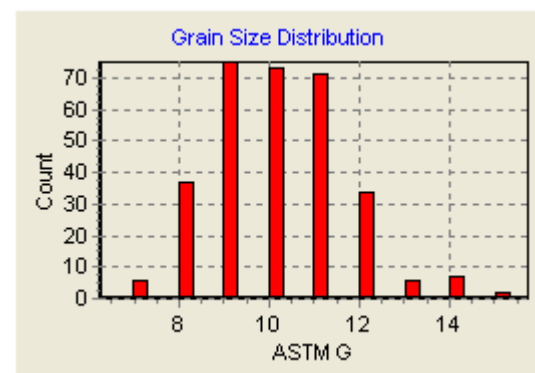
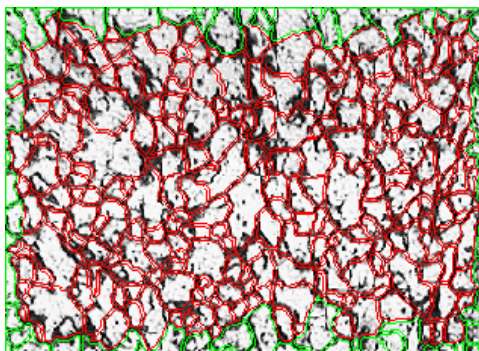
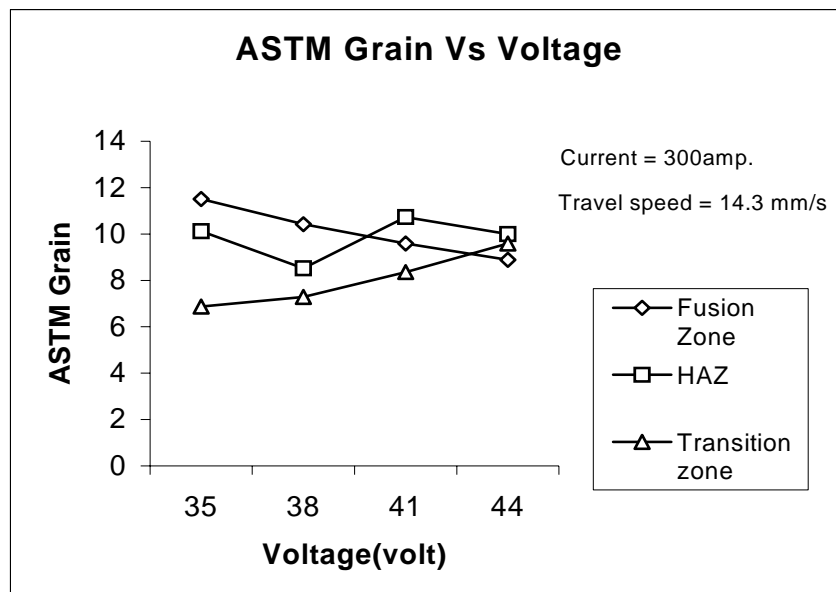


Fig.71 Analyzed pic. of Transition zone sl. no.7

Chart 22. Distribution of grain over area

Result of grain analysis, ASTM Grain = 9.59

The following graph shows the result of increasing current on grain size of Various zone:--



Graph 8. Drawn between ASTM Grain versus Voltage Keeping other parameter constant.

Here we were observed small changes in grain size of HAZ area but in fusion zone the grain size was increased considerably and for transition zone the grain size reduced slightly because of change of pearlite grain into ferrite.

4. CONCLUSIONS:

If we increase the Current in increment of 50 volt (approx.) starting from 510 amp and the voltage in the increment of 3 volt starting from 35 volt, keeping the other parameter constant we are getting the following conclusions:-

❖ **Phase changes in fusion zone:**

Ferrite increases as current increases but no much effect as voltage increases.

Pearlite is following up and down trend as current increases, but increases gradually as voltage increases.

Martensite increases as current increases but decreases as voltage increases

Bainite decreases as current and voltage increases.

❖ **Phase changes in HAZ:**

Ferrite increases as current increases and voltage increases.

Pearlite decreases smoothly as current increases and increases gradually as voltage increases.

Martensite increases as current increases but increases and decreases as voltage increases.

Bainite increases current increases and decreases gradually as voltage increased.

❖ **Phase changes in Transition zone:**

Ferrite decreases as current increases but as very smooth changes as voltage increases.

Pearlite increases as current increases but as very smooth changes as voltage increases.

There is no presence of **Martensite** and **bainite** in the transition zone.

❖ **Grain size changes for fusion zone:**

Coarser grain in final as current increases as compared to increasing voltage.

❖ **Grain size changes for HAZ:**

There is smaller grain in middle of the value of the voltages and finally same size as it was. Increase in current is giving gradual changes in grain size, it is coarsening.

❖ **Grain size changes for HAZ:**

The considerable changes are coming due to increase in voltage as compared to current in the transition zone.

5. SCOPE FOR THE FUTURE WORK:

As we know that the grain size and microstructure fully affecting the mechanical Hardness, Tensile strength and toughness of the welded joints, so the studies in this field will be fruitful for improving the strength of the weldments. By varying the heat input, i.e Increasing the current or voltage we can get the desired microstructure and grain size and thus desired strength.

6. REFERENCES:

- [1.] Garland, J.G., and kikwood, P.R. "*Towards improved submerged arc weld metal (PaA1)*", Mat. Constr. 7:275-283., 1975.
- [2.] Garland, J.G., and kikwood, P.R. "*Towards improved submerged arc weld metal*" (Part 2) Metal. Constr. 7:320-330., 1975.
- [3.] Delong, W.T., "*Ferrite in austenite stainless weld metals*", Welding journal, 53(7): 273s-286s, 1974.
- [4.] Sharma M.K., Ph. D- thesis "*Effect of welding parameters on Mechanical Properties Microstructure and on erosion behaviour of martensite stainless steel*", University of Roorkee, Roorkee, 1996.
- [5.] Munning Schmidt, Van Der Burg., M.A., Hockstra. S., and Den ouden, G.- "*Microstructure and notch toughness of ferritic weld metal*", Philips weld. Reporter, 1984.
- [6.] Dolby R.E., "*Factors controlling weld toughness –the preset position*" (part2 weld-metal), Welding institute research report 14/1976/M, 1976.
- [7.] R.S.Parmar '*Welding Engineering and Technology*' Khannna Publishers, New Delhi (1993).
- [8.] Taylor Lyman (ed) Metals Handbook Vol.1' ASM Metals Park, ohio (1961).
- [9.] Linnert, G.E.; Welding Metallurgy, vol-1., American welding society, New York, 1965.

- [10.] Websites- <http://www.aws.org>, <http://www.science-direct.com> and <http://www.iiwindia.org>.
- [11.] Bob Irving, *The Challenge of welding heat-treatable alloy steels*, weld. J., vol. 74, 1995
- [12.] Easterling, K.E. 1983. *Introduction to the physical metallurgy of welding*. London. U.K., Chapman and Hall.
- [13.] W.G. Cochran, G.M. Cox, *Experimental design*, Asia Publishing House, India.
- [14.] P.T. Houldcraft, *Submerged Arc Welding*, Abington, U.K., 1889.
- [15.] J.F. Lancaster, *The Metallurgy of Welding, Brazing and Soldering*, George Allan and Unwin, London, 1970.

